JPET Fast Forward. Published on May 5, 2022 as DOI: 10.1124/jpet.121.001058
This article has not been copyedited and formatted. The final version may differ from this version.

Title page

Sodium pentobarbital suppresses breast cancer cell growth partly via normalizing microcirculatory hemodynamics and oxygenation in tumors

Qin Wang[1, #], Xueting Liu[2, #], Bingwei Li[3], Xiaojie Yang[1], Wenbao Lu[3], Ailing Li[3], Hongwei Li[3], Xiaoyan Zhang[2, *], Jianqun Han[1, *]

[1]Microhemodynamics Laboratory, Institute of Microcirculation, Chinese Academy of Medical Sciences & Peking Union Medical College, Beijing, China (Q.W., X.Y., H.Q.)

[2]Laboratory of Microvascular Biopathology, Institute of Microcirculation, Chinese Academy of Medical Sciences & Peking Union Medical College, Beijing, China (X.L., X.Z.)

[3]Institute of Microcirculation, Chinese Academy of Medical Sciences & Peking Union Medical College, Beijing, China (B.L., W.L., A.L., H.L.)

[#]These two authors contributed equally to this work.

JPET Fast Forward. Published on May 5, 2022 as DOI: 10.1124/jpet.121.001058
This article has not been copyedited and formatted. The final version may differ from this version.

Running title page

Running title: Sodium pentobarbital suppresses breast cancer

***Correspondence address**

Jianqun Han, Microhemodynamics Laboratory, Institute of Microcirculation, Chinese Academy of Medical Sciences & Peking Union Medical College, Dong Dan San Tiao 5 Hao, Dongcheng District, Beijing 100005, China. Work telephone number: +86-10-65123243, Email: jianqunhan123456@163.com.

Xiaoyan Zhang, Laboratory of Microvascular Biopathology, Institute of Microcirculation, Chinese Academy of Medical Sciences & Peking Union Medical College, Dong Dan San Tiao 5 Hao, Dongcheng District, Beijing 100005, China. Telephone number: +8615811371398, Email: xiaoyan111666@sina.com.

Word count:

Text pages: 31

Tables: 0

Figures: 6

References: 58

Abstract: 245

Introduction: 741

Discussion: 1495

Abbreviations: MBF, microcirculatory blood flow; P. Barbital, sodium pentobarbital; RBC, red blood cell; SO_2, hemoglobin oxygen saturation; THb, total hemoglobin tissue concentration; EPOS, Enhanced Perfusion and Oxygen Saturation; Sk, tumor skin; Ts, tumor surface

Recommended section: Chemotherapy, Antibiotics, and Gene Therapy

JPET Fast Forward. Published on May 5, 2022 as DOI: 10.1124/jpet.121.001058
This article has not been copyedited and formatted. The final version may differ from this version.

ABSTRACT

Breast cancer remains the leading cause of cancer-related death among women worldwidely. Sodium pentobarbital was found to play an inhibitory role in glioma growth in rats. In this study, we aimed to evaluate the effects of sodium pentobarbital on breast cancer growth both in vitro and in vivo, and its impacts on the microcirculatory changes both on skin and tumor surface in mice bearing subcutaneous xenograft. Cell counting assay was used to assess the anti-proliferative effect of sodium pentobarbital on MDA-MB-231 breast cancer cells. Subcutaneous xenograft model was established to study the role of sodium pentobarbital on in vivo tumor growth. Speed-resolved blood perfusion, hemoglobin oxygen saturation (SO_2, %), total hemoglobin tissue concentration (THb, μM), and red blood cell (RBC) tissue fraction (%) were examined simultaneously by using EPOS system, to investigate the effects of sodium pentobarbital on microcirculatory hemodynamics and oxygenation. Sodium pentobarbital suppressed breast tumor growth both in vitro and in vivo. Cutaneous blood flux in nutritive capillaries with low-speed flow was significantly increased in tumor-bearing mice, and high dose sodium pentobarbital treatment cause a reduction in this low-speed blood flux, whereas sodium pentobarbital therapy caused an elevated blood flux in larger microvessels with mid- and high-speed in a dose-dependent manner. Different doses of sodium pentobarbital exerted different actions on SO_2, ctTHb and RBC tissue fraction. Collectively, the inhibitory effect of sodium pentobarbital on breast tumor growth was at least partly associated with its ability to normalize microcirculatory hemodynamics and

JPET Fast Forward. Published on May 5, 2022 as DOI: 10.1124/jpet.121.001058
This article has not been copyedited and formatted. The final version may differ from this version.

oxygenation in tumors.

Significance Statement: This study is the first to demonstrate the inhibiting effect of sodium pentobarbital on breast cancer growth both in vitro and in vivo, and such an inhibition was at least partly associated with its ability to normalize microcirculatory hemodynamics and oxygenation in tumors.

JPET Fast Forward. Published on May 5, 2022 as DOI: 10.1124/jpet.121.001058
This article has not been copyedited and formatted. The final version may differ from this version.

Introduction

Breast cancer is the most common cancer among women accounting for 24% of total new diagnosis and is the leading cause of cancer-related death among women worldwide (Sung et al., 2021). The standard of treatment of breast cancer involves a combination of surgery, chemotherapy, radiation therapy and targeted therapy. However, breast cancer surgery can affect quality of life, fatigue and cognition in patients over the age of 65 years (Harrison et al., 2021). After breast-conserving surgery of hormone receptor-positive (HR^+) breast cancer, standard treatments such as radiation therapy and endocrine therapy is easy to cause treatment-related toxicities and non-cancer related death for old patients (Savard et al., 2021). Chemotherapy drug such as taxanes can cause polyneuropathy (Ciruelos et al., 2019; Ilhan et al., 2017; Park et al., 2013). Effect of targeted drugs for triple-negative breast cancer are limited, and lapatinib showed drug resistance for HER2-positive breast cancer therapy (Sang et al., 2021). There is an urgent need to continue to explore new drugs with anti-tumor potential for breast cancer.

Sodium pentobarbital (P. Barbital) is a fast-acting central depressant acting via γ-aminobutyric acid (GABA) receptors (Mohamed et al., 2020), which is mostly used as an anesthetic agent in animal experiments (Barry et al., 2021; Matsuura and Downie, 2000; Tanioka et al., 2020; Xu et al., 2020). Oral pentobarbital has also been the preferred sedative in pediatric echocardiography in several pediatric departments (Miller et al., 2018; Warden et al., 2010). Notably, some studies reported that phenobarbital exerted inhibitory effects on the development of gliomas in WF rats

JPET Fast Forward. Published on May 5, 2022 as DOI: 10.1124/jpet.121.001058
This article has not been copyedited and formatted. The final version may differ from this version.

treated neonatally with N-ethyl-N-nitrosourea (Naito et al., 1985). Consistently, an *in vitro* study demonstrated that pentobarbital is capable of inhibiting proliferation and migration of malignant glioma cells by arresting cell cycle and interfering microtubule (Xie et al., 2009). However, little is known about the effect of pentobarbital on other types of tumors including breast cancer.

Blood flow is a major driving factor for metabolism and oxygenation in tumor tissues, which, in turn, may have an impact on the effectiveness of some cancer therapies. Tumor blood vessels usually exhibit anomalous morphology characterized by irregular diameters, immature vessel walls and increased vessel tortuosity and permeability, which lead to abnormal microcirculatory blood flow (MBF) (Andleeb et al., 2021). Thus, tumor tissue oxygenation and microcirculatory blood flow are crucial indices for detecting tumor growth and can be used to monitor alterations within the tumor microenvironment and predict neoadjuvant chemotherapy response in both pre-clinical and clinical research (Jing et al., 2019; Koch et al., 2020; Tromberg et al., 2016). There are numerous techniques to measure blood blow and microcirculatory oxygen profiles within tumors, respectively. With regard to blood flow, conventional laser Doppler flowmetry (LDF) is a standard technique for monitoring blood flow noninvasively. LDF provides an indicator of the concentration and velocity of moving blood cells within a region of limited depth, presented in arbitrary units (Smith et al., 2019). Although this technique is of great value in physiological and medicine research, it has not been capable of giving microvascular perfusion in absolute units (Roustit and Cracowski, 2012). In this study, we employed a newly-developed

JPET Fast Forward. Published on May 5, 2022 as DOI: 10.1124/jpet.121.001058
This article has not been copyedited and formatted. The final version may differ from this version.

equipment called EPOS (Enhanced Perfusion and Oxygen Saturation) system, which integrates diffuse reflectance spectroscopy (DRS) and LDF to simultaneously provide absolute measures of both microcirculatory hemodynamics such as velocity-resolved perfusion separated into three speed regions: 0–1 mm/s, 1–10 mm/s and above 10 mm/s (% mm/s) and microcirculatory oxygen profiles including hemoglobin oxygen saturation (SO_2, %), red blood cell (RBC) tissue fraction (%) and oxygenized and reduced hemoglobin tissue concentration (μM) (Fredriksson et al., 2013; Jonasson et al., 2015). Owing to its accessibility, cutaneous microcirculation has emerged as a typical vascular bed for the evaluation of systemic microvascular function and dysfunction (Deegan and Wang, 2019) under various pathological conditions such as diabetes (Feng et al., 2018), hypertension (Concistre et al., 2020), Raynaud's phenomenon (Anderson et al., 2004), and cardiovascular diseases (Agarwal et al., 2012; Shamim-Uzzaman et al., 2002), suggesting the importance of the assessment cutaneous microcirculation in patients to elaborate the underlying pathophysiological mechanisms or to be used as a predictor of treatment response. There are few studies focused on the changes of cutaneous microcirculation in cancer patients (Hsiu et al., 2018; Pedanekar et al., 2019).

Thus, in the present study, we aimed to investigate the potential effects of sodium pentobarbital on the growth of breast cancer both *in vitro* and *in vivo*, and to measure sodium pentobarbital-induced microcirculatory hemodynamics and oxygenation changes in tumor.

JPET Fast Forward. Published on May 5, 2022 as DOI: 10.1124/jpet.121.001058
This article has not been copyedited and formatted. The final version may differ from this version.

Materials and methods

Cell culture and treatment

MDA-MB-231 breast cancer cell line was obtained from National Infrastructure of Cell Line Resource (NICR) (Institute of Basic Medical Science, Chinese Academy of Medical Science and Peking Union Medical College, Beijing, China). The authentication of MDA-MB-231 cell line was performed by using short tandem repeat (STR) typing test (Shanghai Biowing Biotechnology Co. Ltd, China). STR typing profiles showed that 100% matched cell line was found in DSMZ data bank, the name of cell line was MDA-MB-231, and no multiple alleles were found. Cells were maintained in Dulbecco's modified Eagle's medium (DMEM) (Gibco, USA) supplemented with 10% fetal bovine serum (Gibco) in a humidified incubator with 5% CO_2 at 37˚C. For cell treatment, MDA-MB-231 cells were plated in a 12-well plate at a density of with 60% confluence were treated with 0.15, 0.3, 0.6, 1.5 and 3.0 mg/ml sodium pentobarbital (cat# P3761-5G, Sigma-Aldrich; St. Louis, MO, USA) for 40 hours.

Cell counting assay

Cell counting assay was conducted by experienced researchers. Briefly, MDA-MB-231 cells were seeded into 96-well plates at a density of 5×10^3 cells/well in 50 μL DMEM for 24h until 60% confluence. Cells were treated with a series of concentrations of P. Barbital (0.15, 0.3, 0.6, 1.5 and 3.0 mg /ml) for 8, 16, 24, 32, and 40 hours, and then were counted using an IncuCyte Zoom Live-Cell Imaging System

JPET Fast Forward. Published on May 5, 2022 as DOI: 10.1124/jpet.121.001058
This article has not been copyedited and formatted. The final version may differ from this version.

(2015A, Essen Bioscience, Ann Arbor, MI, USA).

In vivo tumor formation assay

Animal care and experimental protocols were in accordance with the Institute for Laboratory Animal Research Guide for Care and Use of Laboratory Animals 8th edition, 2010, National Academies Press, Washington DC, and approved by the Institutional Animal Care and Use Committee at the Institute of Microcirculation, Chinese Academy of Medical Sciences (CAMS). Xenograft model was established by experienced laboratory technicians. Six-week-old female BALB/c nude mice (CAnN.Cg-*Foxn1*^{nu}/Crl, the 1bp (G) deletion of exon 3 of Foxn1 gene on chromosome 11 causes frameshift mutation and the introduction of a stop codon before extraction, leading to premature termination of protein translation) were provided by SPF (Beijing) Biotechnology Co., Ltd. (Beijing, China) and were housed five per cage for 5 days before injection at 24 ± 1°C in a 55 ± 5% humidified atmosphere under a 12h-12h light/dark cycle, and mice are free access to regular diet (Rat & Mouse Growth and Reproduction Formula Feed, Beijing Keao Xieli Feed Co., Ltd, Beijing, China) and drinking water. Approximately 5×10^6 cells at exponential growth stage suspended in 100 μL Matrigel (BD, USA) were inoculated into armpit of each nude mouse. Further, all mice were randomly divided into 4 groups when tumor volume reached 80-100 mm^3: control, 5, 25 and 50mg/kg/day of P. Barbital group. Each group had 6 mice. Control or test P. Barbital (5, 25 or 50mg/kg/day) were injected subcutaneously around the tumor for two consecutive weeks. Calipers were

JPET Fast Forward. Published on May 5, 2022 as DOI: 10.1124/jpet.121.001058
This article has not been copyedited and formatted. The final version may differ from this version.

used to measure the length and width of tumor and tumor volumes were calculated according to the following formula: tumor volume = (length × width^2)/2.

Equipment for measuring microcirculatory hemodynamics and oxygen profiles in tumor

In the present study, we used the PeriFlux 6000 EPOS system (Perimed AB, Järfälla, Stockholm, Sweden), which successfully integrates laser Doppler flowmetry (LDF) and diffuse reflectance spectroscopy (DRS), to accurately measure blood perfusion and oxygen saturation in the microcirculation. The principal advantage of this new technique is that it measures blood perfusion in absolute units, not only qualitatively as when using a standard laser Doppler (Jonasson et al., 2017; Jonasson et al., 2015). Furthermore, it separates different velocity regions within the blood flow termed speed-resolved perfusion. For instance, it is in capacity to distinguish slow nutritive blood flow, which is of great importance for all living cells in the body, from faster flow that is only responsible for transportation (Jonasson et al., 2019). Additionally, it can be used to evaluate the association between flow speed and red blood cell (RBC) oxygen saturation, revealing information about oxygen delivery and uptake into the surrounding tissue. To estimate the microcirculatory parameters, a unique model-based analysis of multimodal measurements is employed. The multilayered tissue model is adapted to the measured signals in real time and the following parameters are obtained from the adapted model: oxygen saturation (SO_2, %); red blood cell (RBC) tissue fraction: gram RBC/100-gram tissue (%); Oxygenized,

JPET Fast Forward. Published on May 5, 2022 as DOI: 10.1124/jpet.121.001058
This article has not been copyedited and formatted. The final version may differ from this version.

reduced and total hemoglobin tissue concentration (μM); Speed-resolved perfusion: gram RBC/100-gram tissue× mm/seconds (% RBC × mm/second). Three different speed regions: < 1 mm/second, 1 to 10 mm/second, and > 10 mm/second.

Measurement protocols

After acclimatizing for 15 min in an experimental room with an ambient temperature of 24 ± 1°C [mean ± standard deviation (SD)] and 50-70% humidity, the tumor-bearing mice were anesthetized with 2% inhaled isoflurane (RWD Life Science, Shenzhen, China) in a 50% mixture of oxygen using a small animal anesthesia machine (Midmark, Dayton, Ohio). Then, mice were in a supine position on a heating pad with continuous inhalation of isoflurane. The probe was placed upon the tumor skin (Sk) steadily by a probe holder (PLT1, Moor Instruments) after the skin was disinfected with 75% ethanol. Researchers measuring microcirculatory hemodynamics and oxygen profiles were trained by technical support from Perimed Technology (Beijing) Co., LTD. The microcirculatory measurements were performed on tumor skin. After the skin was peeled off, the blood perfusion on the exposed tumor surface (Ts) was also measured using the same method. At the end of experiments, mice were euthanized by CO_2 inhalation.

Statistical analysis

Continuous variables are presented as mean ± standard deviation (SD) and categorial variables as percentages. SPSS 21.0 version software (SPSS Inc., Chicago, IL, USA)

JPET Fast Forward. Published on May 5, 2022 as DOI: 10.1124/jpet.121.001058
This article has not been copyedited and formatted. The final version may differ from this version.

was used for data statistical analysis. Two-tailed Student's t-test was used for two-group comparison, and one-way ANOVA analysis was used for statistical comparisons among multiple groups. Figures were generated by using the GraphPad Prism (version 8.0.2; GraphPad Software, San Diego, CA). A $p < 0.05$ was considered as statistical significance.

Results

Sodium pentobarbital suppressed tumor cell proliferation in vitro

As showed in Figure 1, compared with the control group, P. Barbital treatment induced decreased tumor cell viability in a time- and dose-dependent manner. Under normal condition (control group), MDA-MB-231 cells grew fast, cell number doubled at 16 hours, and increased to 4 times after 40 h treatment. Low dose (0.15 mg/ml) P. Barbital exposure slightly suppressed cell viability, demonstrated by the fact that cell number only doubled after 40 h P. Barbital treatment. However, cell viability was obviously suppressed when exposure dose increased to 0.3-3.0 mg/ml. The number of living cells decreased to about 64% in 0.3 mg/ml group and 26% in 0.6 mg/ml group after 40 h treatment. In the highest dose P. Barbital (3.0 mg/ml) group, after 8 hours of treatment, there were very few living cells (about 4%), and no living cells at 16 hours. These data indicate that sodium pentobarbital was supposed to suppress the viability of breast cancer cells *in vitro*.

Sodium pentobarbital inhibited tumor growth in vivo

JPET Fast Forward. Published on May 5, 2022 as DOI: 10.1124/jpet.121.001058
This article has not been copyedited and formatted. The final version may differ from this version.

The effects of P. Barbital at various dose on tumor growth *in vivo* were determined in a subcutaneous xenograft assay using the MDA-MB-231 cells. Our results showed that P. Barbital led to a significant reduction of tumor burden in a concentration-dependent manner, the average tumor weight was reduced significantly after two weeks of 50 mg/kg P. Barbital injection, when compared with the control group (48.64 mg vs 1117.06 mg) (Figure 2C). Consistently, the tumor volume in the low-dose P. Barbital group (5 mg/kg) was similar to that in the control group after one week treatment, and then grew slowly from the ten days after P. Barbital injection compared with the controls. In the medium dosage group (25 mg/kg), the volume of tumors was no more than 100 mm^3 throughout the observation period. In the high dose group (50mg/kg), the average tumor volume shrank to less than 30 mm^3(Figure 2A and 2B). Therefore, these findings explicitly point out that sodium pentobarbital may have a role of inhibiting tumor growth.

Effect of different concentration of sodium pentobarbital on speed resolved perfusion on tumor skin and tumor surface

In the present study, we employed the newly-developed EPOS system, which enables to differentiate the effect in capillaries (low-speed flow) from those in larger microvascular vessels (high-speed flow) such as venules and arterioles using the velocity-resolved quantitative measure, to monitor microcirculatory blood flow for the first time in tumor, and this system has already been used in determining the microcirculatory velocity distribution in patients with type 2 diabetes (Fredriksson et

JPET Fast Forward. Published on May 5, 2022 as DOI: 10.1124/jpet.121.001058
This article has not been copyedited and formatted. The final version may differ from this version.

al., 2010). Analysis of association between flow velocity and vessel type may offer novel insights into the microvascular function.

As Figure 3A and 4A (left) presented, an increased blood flux occurred in low-speed regions (<1 mm/s) on tumor skin (Sk) compared with that in control skin ($P<0.0001$), and the lowest dose (5 mg/kg) of P. Barbital treatment remarkably elevated the blood flux in the low-speed region on tumor skin ($P<0.0001$), however, when exposure dose of P. Barbital increased to 10 times (50 mg/kg), the blood flux in the low-speed region reduced significantly on tumor skin ($P<0.0001$). With regard to perfusion in the mid- (1-10 mm/s) and high-speed (>10 mm/s) regions, a large decrease was observed on tumor skin when compared with the control skin (both $P<0.0001$ in the mid- and high-speed regions), and P. Barbital stimulation significantly increased the blood flux in the mid- and high-speed regions in a concentration dependent manner (Figure 3B and 4B, left, 3C and 4C, left). In addition, total perfusion in all speed regions were significantly lower on tumor skin compared to that in the control skin, and P. Barbital treatment significantly improved total perfusion on tumor skin (Figure 3D and 4D, left). Furthermore, mean percentage of total perfusion for the three perfusion components was also compared, the results showed that the mean percentage of total perfusion in low-speed region significantly increased on tumor skin compared with that in the control skin, and medium and high concentrations of P. Barbital stimulation led to a notable drop in mean percentage of total perfusion in low-speed region on tumor skin. Consistent with the findings on blood flux on tumor skin, P. Barbital treatment also significantly increased the blood flux in the mid-, high-speed regions

JPET Fast Forward. Published on May 5, 2022 as DOI: 10.1124/jpet.121.001058
This article has not been copyedited and formatted. The final version may differ from this version.

and total perfusion in all speed regions on tumor surface (Ts), in a dose-dependent manner (Figure 3B and 4B, right, right, 3C and 4C, right). However, there was a slightly different impact of P. Barbital on blood flux in low-speed regions (<1 mm/s) between Sk and Ts, as shown in Figure 3A and 4A, P. Barbital increased blood flux in low-speed regions (<1 mm/s) on tumor surface in a dose-dependent manner.

Taken together, these data suggest that 50 mg/kg P. Barbital is effective enough to reduce blood perfusion in nutritive capillaries with low-speed flow on tumor skin, and that P. Barbital has excellent efficacy in increasing blood perfusion in larger microvascular vessels with high-speed flow on tumor skin in a dose-dependent manner. P. Barbital stimulation led to an elevated blood flux in all three speed regions on tumor surface.

Effect sodium pentobarbital on oxyhemoglobin saturation, tissue concentration of total hemoglobin and RBC tissue fraction on tumor skin and tumor surface

Tumoral metabolic measurements such as tissue concentrations of oxygenized hemoglobin (ctO_2Hb), deoxygenized hemoglobin (ctHHb), total hemoglobin (ctTHb) and oxyhemoglobin saturation (SO_2) are directly associated with tumor metabolism and vascular features. The difference between tumors and healthy tissue is expected to be achieved by comparing ctTHb and SO_2, thus, in the present study, we investigated whether P. Barbital had an effect on SO_2 and ctTHb in both tumor skin and tumor surface. Quantitative analysis revealed a notable reduction in SO_2 on tumor skin compared to the normal skin (38.77% vs. 52.19%, P<0.0001), and low dose (5 mg/kg)

JPET Fast Forward. Published on May 5, 2022 as DOI: 10.1124/jpet.121.001058
This article has not been copyedited and formatted. The final version may differ from this version.

P. Barbital treatment resulted in a moderate increase in SO_2 on tumor skin compared to untreated tumors (40.3% vs. 38.77%, P=0.017, Figure 5A and 6A). Interestingly, mid- and high dose (25 mg/kg and 50 mg/kg) P. Barbital treatment further reduced SO_2 on tumor skin when compared with untreated tumors. Consistently, low dose P. Barbital exposure also mildly increased SO_2 on tumor surface compared to untreated tumor surface (50.1% vs. 48.6%, P=0.0048), and mid- and high dose P. Barbital treatment further decreased SO_2 on tumor surface (44.69% vs. 42.49% vs. 48.6%, both P<0.0001, Figure 5B and 6B). Furthermore, tumor skin exhibited significant raise of ctTHb compared to control skin (16.81 μM vs. 10.13 μM, P<0.0001), and mid- and high-level P. Barbital exposure reduced ctTHb on tumor skin to normal level compared to the skin of untreated tumors (7.95 μM vs. 9.69 μM vs. 16.81 μM, both P<0.0001, Figure 5C and 6C). Similarly, P. Barbital treatment significantly decreased ctTHb on tumor surface when compared with untreated tumor surface at a dose-dependent manner (35.39 μM vs. 31.79 μM vs. 22.37 μM vs. 39.9 μM, Figure 5D and 6D). In the present study, we also assessed the effect of different doses of P. Barbital treatment on RBC tissue fraction on tumor skin and tumor surface. As shown in Figure 5E and 6E, RBC tissue fraction was much higher on tumor skin compared to control skin (0.33% vs. 0.19%), and application of low dose P. Barbital further increased the RBC tissue fraction. Instead, mid- and high dose of P. Barbital exposure significantly reduced RBC tissue fraction on tumor skin compared to untreated tumors (0.19% vs. 0.15% vs. 0.33%). The same phenomenon occurred on tumor surface, as Figure 5F and 6F presented, low dose P. Barbital treatment caused elevated RBC

JPET Fast Forward. Published on May 5, 2022 as DOI: 10.1124/jpet.121.001058
This article has not been copyedited and formatted. The final version may differ from this version.

tissue fraction on tumor surface compared to untreated tumors, and application of high dose P. Barbital resulted in a significant drop in RBC tissue fraction on tumor surface when compared with untreated tumors. Collectively, these results revealed the opposite effect of different dose of P. Barbital on ctO_2Hb, ctTHb and RBC tissue fraction both on tumor skin and tumor surface.

Discussion

In the present study, we observed that (1) P. Barbital suppressed breast tumor growth both *in vitro* and *in vivo*; (2) high dose (50 mg/kg) P. Barbital treatment cause a significant reduction in blood flux in nutritive capillaries with low-speed flow on tumor skin, whereas P. Barbital consumption resulted in an increased blood flux in larger micro vessels with high-speed flow in a dose-dependent manner. P. Barbital treatment led to an elevated blood flux in all three speed regions on tumor surface; (3) different doses of P. Barbital play distinct roles in ctO_2Hb, ctTHb and RBC tissue fraction both on tumor skin and tumor surface. The method used in this study provides data in absolute units rather than presenting microcirculatory parameters in arbitrary units in many previous literatures.

Heterogeneity of tumors including breast cancer is the principal cause of acquired treatment resistance, recurrence and progression (AlSendi et al., 2021; Polyak, 2011; Skowron et al., 2021; Zardavas et al., 2015). Reducing treatment-related side effects is another major challenge for clinicians (Berliere et al., 2021). Effective drugs or adjuvant drugs with less adverse effect for breast cancer are currently still being

JPET Fast Forward. Published on May 5, 2022 as DOI: 10.1124/jpet.121.001058
This article has not been copyedited and formatted. The final version may differ from this version.

explored.

Sodium pentobarbital, a short-acting GABAA-receptor potentiator, which is usually used as a pre-operative anesthetic in severe insomnia and seizure epilepsy emergency management, can cause a loss of consciousness and cardiovascular depression (Olsen and Li, 2011; Priest and Geisbuhler, 2015; Sierra-Valdez et al., 2016). A study from Xie *et al* showed that anesthetic pentobarbital was capable of suppressing proliferation and migration of C6 malignant glioma cells in a concentration-dependent manner (Xie et al., 2009). Anesthetic sevoflurane was also shown to exert anti-proliferative and anti-metastatic effects on osteosarcoma cells by inactivating PI3K/AKT pathway (Gao et al., 2019). In accordance with these findings, in this study, we demonstrated that sodium pentobarbital significantly inhibited the growth of breast cancer in a dose-dependent manner both *in vitro* and *in vivo*. Besides, the doses of sodium pentobarbital used in the current experiment (less than 50 mg/kg in animal model) is safe and reliable, and is not associated with obvious side effects.

In the current study, we examined the differences of cutaneous microcirculatory parameters between tumor-bearing mice and healthy mice, and assessed the influences of sodium pentobarbital on cutaneous microcirculation. We employed a new LDF signal analysis, which enables separating the blood flow into three flow speed regions to correlate differences in the speed distribution to specific vessel types, as large vessels such as arterioles, venules, and arteriovenous shunts are commonly associated with higher blood flow velocity than smaller vessels which are mainly nutritive capillaries (Fredriksson et al., 2010). We have shown that the elevated blood perfusion

JPET Fast Forward. Published on May 5, 2022 as DOI: 10.1124/jpet.121.001058
This article has not been copyedited and formatted. The final version may differ from this version.

occurred in vessels with a velocity<1 mm/s on tumor skin due to higher metabolic demand when compared with the control skin, and high dose (50 mg/kg) P. Barbital treatment attenuated the increased blood perfusion for low-speed region on tumor skin, suggesting an inhibiting role for high dose of P. Barbital. These results were in consistent with the findings by Tanvi Pedanekar *et al*, who have revealed a notable decrease in the blood flux on the skin surface along with the smaller tumor size in patients with good therapeutic response (Pedanekar et al., 2019). Similarly, the highest level of skin blood flow has been observed in patients with breast cancer compared to benign breast and healthy controls (Seifalian et al., 1995). On the contrary, a significant reduction of blood perfusion was observed in larger vessels with mid- and high-speed on tumor skin, and P. Barbital treatment increased the blood perfusion for mid- and high-speed regions on tumor skin. These results can be explained at least partially by the fact that the larger-vessels with high-speed perfusion was crucial to the endothelial function, under some pathological conditions such diabetes, endothelial injury occurred resulting in inhibition of NO-mediated vasodilation and reduction of high-speed perfusion (Bergstrand et al., 2018). P. Barbital can increase the blood perfusion for mid- and high-speed regions on tumor skin in a dose dependent manner.

With regard to blood perfusion on tumor surface, our findings indicated that P. Barbital markedly increased the blood perfusion for all three-speed regions compared to untreated tumors. These findings were consistent with previous study, which indicated that low tumor blood flow could be a crucial feature of rectal cancer

JPET Fast Forward. Published on May 5, 2022 as DOI: 10.1124/jpet.121.001058
This article has not been copyedited and formatted. The final version may differ from this version.

aggressiveness, and higher tumor blood flow was a predictor of good neoadjuvant treatment response (Bakke et al., 2020). The underlying mechanism for the above findings may be related to the fact that tumor angiogenesis is extraordinarily active, leading to abnormal vascular structure including tortuosity, dilation and inadequate pericyte coverage, and subsequent vascular dysfunction including insufficient blood flow. P. Barbital treatment can normalize tumor vasculature, then increase blood perfusion in tumor tissue. However, Peter Vaupel *et al* have shown that the overall mean flow in prostate cancer (PC) tissue is approximately three times higher than that in normal prostate (NP) tissue (Vaupel and Kelleher, 2013). The conflicting results are at least in part due to the difference in measurement positions (Vinik et al., 2001) and instrumentation (Fredriksson et al., 2009) used .

Tumoral tissue oxygen saturation (SO_2) has been considered as an early predictive factor of tumor response to treatment, and lower SO_2 is associated with non-complete pathological response to treatment (Cochran et al., 2018; Ueda et al., 2012). EPOS system in this study revealed a rise on tumor surface for SO_2 and a reduction for the concentration total hemoglobin (ctTHb) following low dose (5 mg/kg) P. Barbital therapy, and mid- and high dose of P. Barbital treatment further reduced ctTHb. Increased SO_2 represents less tumoral hypoxic, and decreased ctTHb indicates smaller blood volume of the tumors. Previous studies also demonstrated that mean ctTHb in breast tumors was about 3.5 times higher than that in normal counterpart due to larger blood volume, and ctTHb over SO_2 further distinguished between tumoral and normal breast tissue (Grosenick et al., 2005). Thus, tumor growth inhibition effect of P.

JPET Fast Forward. Published on May 5, 2022 as DOI: 10.1124/jpet.121.001058
This article has not been copyedited and formatted. The final version may differ from this version.

Barbital is at least in part due to its role in decreasing ctTHb on tumor surface. Interestingly, in this study, we found that mid- and high-dose P. Barbital treatment further exacerbated the reduction in tumor SO_2, and the underlying mechanisms need to be further explored. To the best of our knowledge, this is the first study to assess the differences of cutaneous SO_2 and ctTHb between tumor-bearing and healthy mice. The SO_2 and ctTHb in cutaneous blood are thought to be strongly associated with cutaneous metabolism (Nagashima et al., 2000). In untreated tumor-bearing group, a decline of cutaneous SO_2 was observed, together with an increase in ctTHb compared to healthy controls. P. Barbital treatment resulted in a notable increase for cutaneous SO_2 in a dose-dependent manner, and mid- and high-dose P. Barbital therapy caused marked reduction for cutaneous ctTHb. Like SO_2, red blood cell (RBC) tissue fraction is a crucial parameter reflecting microvascular function (Ewerlof et al., 2021). Moreover, quantifying blood flow, oxygenation and RBC tissue fraction simultaneously from the same position of the tissue may offer an optimal assessment of the microcirculation under physiopathological conditions. However, as far as we know, there have been few studies estimating the association between RBC tissue fraction and microvascular function in diseases (Jonasson et al., 2017). In the present study, we observed the increased cutaneous RBC tissue fraction in tumor-bearing mice compared to healthy controls, and 5 mg/kg P. Barbital treatment caused further increase of RBC tissue fraction both on tumor skin and tumor surface. On the contrary, 25 mg/kg and 50 mg/kg P. Barbital therapy significantly reduced RBC tissue fraction both on tumor skin and tumor surface. Although EPOS system is a relatively new

JPET Fast Forward. Published on May 5, 2022 as DOI: 10.1124/jpet.121.001058
This article has not been copyedited and formatted. The final version may differ from this version.

device, it uses diffuse reflectance spectroscopy (DRS), which is a not common optical method in recent years, to quantify the SO_2. The prominent feature of EPOS system is that it combines the DRS and laser Doppler flowmetry (LDF) into one joint model to increase the credibility of the method analyzing data from the two techniques separately.

This study has some limitations. Firstly, we observed the antitumor effect of P. Barbital on tumor growth and its role in regulating blood perfusion and oxygenation both on skin and tumor surface. However, the molecular mechanisms underlying these observations have not been explored in the present study and need to be further investigated. Secondly, whether P. Barbital has similar effects on other types of tumors also needs to be further studied. Thirdly, this study showed the opposite effects of P. Barbital on oxygen saturation and total hemoglobin on tumor skin, other technologies should be used to verify these effects in further studies.

In conclusion, we demonstrated the anticancer effect of P. Barbital. Firstly, P. Barbital suppresses breast tumor growth both *in vitro* and *in vivo* in a dose-dependent manner. Secondly, P. Barbital inhibited breast tumor growth at least partly through normalizing both cutaneous and tumor surface blood perfusion. Thirdly, different doses of P. Barbital play distinct roles in ctO_2Hb, ctTHb and RBC tissue fraction both on tumor skin and tumor surface.

Acknowledgments

This work got help from Mingming Liu and Yuan Li, both of whom are from Institute

of Microcirculation, Chinese Academy of Medical Sciences & Peking Union Medical College, in the use and maintenance of the EPOS system.

Authorship Contributions

Participated in research design: Xiaoyan Zhang and Qin Wang.

Conducted experiments: Xiaoyan Zhang, Qin Wang, Xueting Liu, Bingwei Li, Xiaojie Yang, Wenbao Lu, Ailing Li, Hongwei Li and Jianqun Han.

Performed data analysis: Qin Wang, Xiaoyan Zhang and Xueting Liu.

Wrote or contributed to the writing of the manuscript: Qin Wang, Xiaoyan Zhang and Jianqun Han.

JPET Fast Forward. Published on May 5, 2022 as DOI: 10.1124/jpet.121.001058
This article has not been copyedited and formatted. The final version may differ from this version.

References

Agarwal SC, Allen J, Murray A and Purcell IF (2012) Laser Doppler assessment of dermal circulatory changes in people with coronary artery disease. *Microvasc Res* **84**:55-59.

AlSendi M, O'Reilly D, Zeidan YH and Kelly CM (2021) Oligometastatic breast cancer: Are we there yet? *Int J Cancer* **149**:1520-1528.

Anderson ME, Moore TL, Lunt M and Herrick AL (2004) Digital iontophoresis of vasoactive substances as measured by laser Doppler imaging--a non-invasive technique by which to measure microvascular dysfunction in Raynaud's phenomenon. *Rheumatology (Oxford)* **43**:986-991.

Andleeb F, Katta N, Gruslova A, Muralidharan B, Estrada A, McElroy AB, Ullah H, Brenner AJ and Milner TE (2021) Differentiation of Brain Tumor Microvasculature From Normal Vessels Using Optical Coherence Angiography. *Lasers Surg Med*.

Bakke KM, Meltzer S, Grovik E, Negard A, Holmedal SH, Gjesdal KI, Bjornerud A, Ree AH and Redalen KR (2020) Sex Differences and Tumor Blood Flow from Dynamic Susceptibility Contrast MRI Are Associated with Treatment Response after Chemoradiation and Long-term Survival in Rectal Cancer. *Radiology* **297**:352-360.

Barry EF, O'Neill J, Abdulla MH and Johns EJ (2021) The renal excretory responses to acute renal interstitial angiotensin (1-7) infusion in anaesthetised spontaneously hypertensive rats. *Clin Exp Pharmacol Physiol*.

Bergstrand S, Morales MA, Coppini G, Larsson M and Stromberg T (2018) The relationship between forearm skin speed-resolved perfusion and oxygen saturation, and finger arterial pulsation amplitudes, as indirect measures of endothelial function. *Microcirculation* **25**.

Berliere M, Piette N, Bernard M, Lacroix C, Gerday A, Samartzi V, Coyette M, Roelants F, Docquier MA, Touil N, Watremez C, Piette P and Duhoux FOP (2021) Hypnosis Sedation Reduces the Duration of Different Side Effects of Cancer Treatments in Breast Cancer Patients Receiving Neoadjuvant Chemotherapy. *Cancers (Basel)* **13**.

Ciruelos E, Apellaniz-Ruiz M, Cantos B, Martinez-Janez N, Bueno-Muino C, Echarri MJ, Enrech S, Guerra JA, Manso L, Pascual T, Dominguez C, Gonzalo JF, Sanz JL, Rodriguez-Antona C and Sepulveda JM (2019) A Pilot, Phase II, Randomized, Open-Label Clinical Trial Comparing the Neurotoxicity of Three Dose Regimens of Nab-Paclitaxel to That of Solvent-Based Paclitaxel as the First-Line Treatment for Patients with Human Epidermal Growth Factor Receptor Type 2-Negative Metastatic Breast Cancer. *Oncologist* **24**:e1024-e1033.

Cochran JM, Busch DR, Leproux A, Zhang Z, O'Sullivan TD, Cerussi AE, Carpenter PM, Mehta RS, Roblyer D, Yang W, Paulsen KD, Pogue B, Jiang S, Kaufman PA, Chung SH, Schnall M, Snyder BS, Hylton N, Carp SA, Isakoff SJ, Mankoff D, Tromberg BJ and Yodh AG (2018) Tissue oxygen saturation predicts response to breast cancer neoadjuvant chemotherapy within 10 days of treatment. *J Biomed Opt* **24**:1-11.

Concistre A, Petramala L, Bonvicini M, Gigante A, Collalti G, Pellicano C, Olmati F, Iannucci G, Soldini M, Rosato E and Letizia C (2020) Comparisons of skin microvascular changes in patients with primary aldosteronism and essential hypertension. *Hypertens Res* **43**:1222-1230.

Deegan AJ and Wang RK (2019) Microvascular imaging of the skin. *Phys Med Biol* **64**:07TR01.

Ewerlof M, Salerud EG, Stromberg T and Larsson M (2021) Estimation of skin microcirculatory hemoglobin oxygen saturation and red blood cell tissue fraction using a multispectral snapshot

imaging system: a validation study. *J Biomed Opt* **26**.

Feng W, Shi R, Zhang C, Liu S, Yu T and Zhu D (2018) Visualization of skin microvascular dysfunction of type 1 diabetic mice using in vivo skin optical clearing method. *J Biomed Opt* **24**:1-9.

Fredriksson I, Burdakov O, Larsson M and Stromberg T (2013) Inverse Monte Carlo in a multilayered tissue model: merging diffuse reflectance spectroscopy and laser Doppler flowmetry. *J Biomed Opt* **18**:127004.

Fredriksson I, Larsson M, Nystrom FH, Lanne T, Ostgren CJ and Stromberg T (2010) Reduced arteriovenous shunting capacity after local heating and redistribution of baseline skin blood flow in type 2 diabetes assessed with velocity-resolved quantitative laser Doppler flowmetry. *Diabetes* **59**:1578-1584.

Fredriksson I, Larsson M and Stromberg T (2009) Measurement depth and volume in laser Doppler flowmetry. *Microvasc Res* **78**:4-13.

Gao K, Su Z, Liu H and Liu Y (2019) Anti-proliferation and anti-metastatic effects of sevoflurane on human osteosarcoma U2OS and Saos-2 cells. *Exp Mol Pathol* **108**:121-130.

Grosenick D, Wabnitz H, Moesta KT, Mucke J, Schlag PM and Rinneberg H (2005) Time-domain scanning optical mammography: II. Optical properties and tissue parameters of 87 carcinomas. *Phys Med Biol* **50**:2451-2468.

Harrison CA, Parks RM and Cheung KL (2021) The impact of breast cancer surgery on functional status in older women - A systematic review of the literature. *Eur J Surg Oncol* **47**:1891-1899.

Hsiu H, Chen CT, Hung SH, Chen GZ and Huang YL (2018) Differences in time-domain and spectral indexes of skin-surface laser-Doppler signals between controls and breast-cancer subjects. *Clin Hemorheol Microcirc* **69**:371-381.

Ilhan E, Chee E, Hush J and Moloney N (2017) The prevalence of neuropathic pain is high after treatment for breast cancer: a systematic review. *Pain* **158**:2082-2091.

Jing X, Yang F, Shao C, Wei K, Xie M, Shen H and Shu Y (2019) Role of hypoxia in cancer therapy by regulating the tumor microenvironment. *Mol Cancer* **18**:157.

Jonasson H, Bergstrand S, Nystrom FH, Lanne T, Ostgren CJ, Bjarnegard N, Fredriksson I, Larsson M and Stromberg T (2017) Skin microvascular endothelial dysfunction is associated with type 2 diabetes independently of microalbuminuria and arterial stiffness. *Diab Vasc Dis Res* **14**:363-371.

Jonasson H, Fredriksson I, Larsson M and Stromberg T (2019) Validation of speed-resolved laser Doppler perfusion in a multimodal optical system using a blood-flow phantom. *J Biomed Opt* **24**:1-8.

Jonasson H, Fredriksson I, Pettersson A, Larsson M and Stromberg T (2015) Oxygen saturation, red blood cell tissue fraction and speed resolved perfusion - A new optical method for microcirculatory assessment. *Microvasc Res* **102**:70-77.

Koch KU, Mikkelsen IK, Aanerud J, Espelund US, Tietze A, Oettingen GV, Juul N, Nikolajsen L, Ostergaard L and Rasmussen M (2020) Ephedrine versus Phenylephrine Effect on Cerebral Blood Flow and Oxygen Consumption in Anesthetized Brain Tumor Patients: A Randomized Clinical Trial. *Anesthesiology* **133**:304-317.

Matsuura S and Downie JW (2000) Effect of anesthetics on reflex micturition in the chronic cannula-implanted rat. *Neurourol Urodyn* **19**:87-99.

Miller JW, Ding L, Gunter JB, Lam JE, Lin EP, Paquin JR, Li BL, Spaeth JP, Kreeger RN, Divanovic A,

Mahmoud M and Loepke AW (2018) Comparison of Intranasal Dexmedetomidine and Oral Pentobarbital Sedation for Transthoracic Echocardiography in Infants and Toddlers: A Prospective, Randomized, Double-Blind Trial. *Anesth Analg* **126**:2009-2016.

Mohamed AS, Hosney M, Bassiony H, Hassanein SS, Soliman AM, Fahmy SR and Gaafar K (2020) Sodium pentobarbital dosages for exsanguination affect biochemical, molecular and histological measurements in rats. *Sci Rep* **10**:378.

Nagashima Y, Yada Y, Hattori M and Sakai A (2000) Development of a new instrument to measure oxygen saturation and total hemoglobin volume in local skin by near-infrared spectroscopy and its clinical application. *Int J Biometeorol* **44**:11-19.

Naito M, Aoyama H and Ito A (1985) Inhibitory effect of phenobarbital on the development of gliomas in WF rats treated neonatally with N-ethyl-N-nitrosourea. *J Natl Cancer Inst* **74**:725-728.

Olsen RW and Li GD (2011) GABA(A) receptors as molecular targets of general anesthetics: identification of binding sites provides clues to allosteric modulation. *Can J Anaesth* **58**:206-215.

Park SB, Goldstein D, Krishnan AV, Lin CS, Friedlander ML, Cassidy J, Koltzenburg M and Kiernan MC (2013) Chemotherapy-induced peripheral neurotoxicity: a critical analysis. *CA Cancer J Clin* **63**:419-437.

Pedanekar T, Kedare R and Sengupta A (2019) Monitoring tumor progression by mapping skin microcirculation with laser Doppler flowmetry. *Lasers Med Sci* **34**:61-77.

Polyak K (2011) Heterogeneity in breast cancer. *J Clin Invest* **121**:3786-3788.

Priest SM and Geisbuhler TP (2015) Injectable sodium pentobarbital: Stability at room temperature. *J Pharmacol Toxicol Methods* **76**:38-42.

Roustit M and Cracowski JL (2012) Non-invasive assessment of skin microvascular function in humans: an insight into methods. *Microcirculation* **19**:47-64.

Sang X, Li L, Rui C, Liu Y, Liu Z, Tao Z, Cheng H and Liu P (2021) Induction of EnR stress by Melatonin enhances the cytotoxic effect of Lapatinib in HER2-positive breast cancer. *Cancer Lett* **518**:82-93.

Savard MF, Clemons M, Hutton B, Jemaan Alzahrani M, Caudrelier JM, Vandermeer L, Liu M, Saunders D, Sienkiewicz M, Stober C, Cole K, Shorr R, Arnaout A and Chang L (2021) De-escalating adjuvant therapies in older patients with lower risk estrogen receptor-positive breast cancer treated with breast-conserving surgery: A systematic review and meta-analysis. *Cancer Treat Rev* **99**:102254.

Seifalian AM, Chaloupka K and Parbhoo SP (1995) Laser Doppler perfusion imaging--a new technique for measuring breast skin blood flow. *Int J Microcirc Clin Exp* **15**:125-130.

Shamim-Uzzaman QA, Pfenninger D, Kehrer C, Chakrabarti A, Kacirotti N, Rubenfire M, Brook R and Rajagopalan S (2002) Altered cutaneous microvascular responses to reactive hyperaemia in coronary artery disease: a comparative study with conduit vessel responses. *Clin Sci (Lond)* **103**:267-273.

Sierra-Valdez FJ, Ruiz-Suarez JC and Delint-Ramirez I (2016) Pentobarbital modifies the lipid raft-protein interaction: A first clue about the anesthesia mechanism on NMDA and GABAA receptors. *Biochim Biophys Acta* **1858**:2603-2610.

Skowron MA, Oing C, Bremmer F, Strobel P, Murray MJ, Coleman N, Amatruda JF, Honecker F, Bokemeyer C, Albers P and Nettersheim D (2021) The developmental origin of cancers defines basic principles of cisplatin resistance. *Cancer Lett* **519**:199-210.

JPET Fast Forward. Published on May 5, 2022 as DOI: 10.1124/jpet.121.001058
This article has not been copyedited and formatted. The final version may differ from this version.

Smith KJ, Argarini R, Carter HH, Quirk BC, Haynes A, Naylor LH, McKirdy H, Kirk RW, McLaughlin RA and Green DJ (2019) Novel Noninvasive Assessment of Microvascular Structure and Function in Humans. *Med Sci Sports Exerc* **51**:1558-1565.

Sung H, Ferlay J, Siegel RL, Laversanne M, Soerjomataram I, Jemal A and Bray F (2021) Global Cancer Statistics 2020: GLOBOCAN Estimates of Incidence and Mortality Worldwide for 36 Cancers in 185 Countries. *CA Cancer J Clin* **71**:209-249.

Tanioka M, Park WK, Park J, Lee JE and Lee BH (2020) Lipid Emulsion Improves Functional Recovery in an Animal Model of Stroke. *Int J Mol Sci* **21**.

Tromberg BJ, Zhang Z, Leproux A, O'Sullivan TD, Cerussi AE, Carpenter PM, Mehta RS, Roblyer D, Yang W, Paulsen KD, Pogue BW, Jiang S, Kaufman PA, Yodh AG, Chung SH, Schnall M, Snyder BS, Hylton N, Boas DA, Carp SA, Isakoff SJ, Mankoff D and investigators A (2016) Predicting Responses to Neoadjuvant Chemotherapy in Breast Cancer: ACRIN 6691 Trial of Diffuse Optical Spectroscopic Imaging. *Cancer Res* **76**:5933-5944.

Ueda S, Roblyer D, Cerussi A, Durkin A, Leproux A, Santoro Y, Xu S, O'Sullivan TD, Hsiang D, Mehta R, Butler J and Tromberg BJ (2012) Baseline tumor oxygen saturation correlates with a pathologic complete response in breast cancer patients undergoing neoadjuvant chemotherapy. *Cancer Res* **72**:4318-4328.

Vaupel P and Kelleher DK (2013) Blood flow and oxygenation status of prostate cancers. *Adv Exp Med Biol* **765**:299-305.

Vinik AI, Erbas T, Park TS, Pierce KK and Stansberry KB (2001) Methods for evaluation of peripheral neurovascular dysfunction. *Diabetes Technol Ther* **3**:29-50.

Warden CN, Bernard PK and Kimball TR (2010) The efficacy and safety of oral pentobarbital sedation in pediatric echocardiography. *J Am Soc Echocardiogr* **23**:33-37.

Xie J, Li Y, Huang Y, Qiu P, Shu M, Zhu W, Ou Y and Yan G (2009) Anesthetic pentobarbital inhibits proliferation and migration of malignant glioma cells. *Cancer Lett* **282**:35-42.

Xu SF, Du GH, Abulikim K, Cao P and Tan HB (2020) Verification and Defined Dosage of Sodium Pentobarbital for a Urodynamic Study in the Possibility of Survival Experiments in Female Rat. *Biomed Res Int* **2020**:6109497.

Zardavas D, Irrthum A, Swanton C and Piccart M (2015) Clinical management of breast cancer heterogeneity. *Nat Rev Clin Oncol* **12**:381-394.

Footnotes

This research was funded by the Institute of Microcirculation, PUMC Fundamental Research Fund, Grant/ Award Numbers: WXH2020-02.

Conflicts of Interest

The authors declare no conflict of interest

JPET Fast Forward. Published on May 5, 2022 as DOI: 10.1124/jpet.121.001058
This article has not been copyedited and formatted. The final version may differ from this version.

Legends for Figures

Figure 1. Sodium pentobarbital inhibited the proliferation of breast cancer cells *in vitro*. A, an equal amount of MDA-MB-231 breast cancer cells were treated with 0.15 mg/ml, 0.3 mg/ml, 0.6 mg/ml, 1.5 mg/ml and 3.0 mg/ml of sodium pentobarbital at different time points, respectively. Images are representative of cells under light microscope. Bar: 300 μm. B, cell number of A was determined by the cell counting assay using an IncuCyte Zoom Live-Cell Imaging System, and the proliferation rate of sodium pentobarbital was expressed as a fold of cell counts at 0 hour. ****P ≤0.0001; **P ≤0.01; *P ≤0.05 vs. Control group.

Figure 2. Sodium pentobarbital suppressed tumor growth *in vivo* in a time- and dose-dependent manner. A, Morphologic characteristics of xenograft tumors from Control, 5mg/kg, 25mg/kg and 50mg/kg P. barbital group. B, the effect of sodium pentobarbital on tumor growth was investigated in a subcutaneous tumor model, and tumor growth was expressed as a tumor volume. Data points represent the mean±S.D. ***P ≤0.001; **P ≤0.01; *P ≤0.05 vs. Control group. C, changes in tumor growth rate were also reflected by final tumor weights after two weeks of sodium pentobarbital treatment. Data represent the mean±S.D. ****P ≤0.0001; **P ≤0.01 vs. Control group.

Figure 3. Effects of sodium pentobarbital on blood perfusion both on tumor skin (Sk) and tumor surface (Ts) as presented with line charts. Blood perfusion in

JPET Fast Forward. Published on May 5, 2022 as DOI: 10.1124/jpet.121.001058
This article has not been copyedited and formatted. The final version may differ from this version.

percent RBC times their speed (divided into speed regions 0–1 mm/s (A), 1–10 mm/s (B), above 10 mm/s (C) and total perfusion (D) both on Sk (left) and Ts (right) was shown in different groups: Control, Tumor, 5, 25 and 50 mg/kg P. Barbital group.

Figure 4. Different influences of sodium pentobarbital on blood perfusion for three-speed regions both on tumor skin and tumor surface. Blood perfusion for low-speed region (0-1 mm/s) (A), mid-speed region (1-10 mm/s) (B), high-speed region (>10 mm/s) on skin (Sk, left) and tumor surface (Ts, right) was evaluated by using EPOS system in tumor-bearing mice treated with different doses of sodium pentobarbital and healthy controls. Data are presented as the mean±S.D. ****P ≤0.0001; **P ≤0.01; *P ≤0.05.

Figure 5. Effects of sodium pentobarbital on oxygenation both on tumor skin (Sk) and tumor surface (Ts) as presented with line charts. Oxyhemoglobin saturation (SO_2) (A, B), tissue concentration of total hemoglobin (ctTHb) (C, D), and red blood cell (RBC) tissue fraction (E, F) both on Sk (A, C and E) and Ts (B, D and F) in different groups: Control, Tumor, 5, 25 and 50 mg/kg P. Barbital group were shown by line charts.

Figure 6. Different concentrations of sodium pentobarbital have different roles on oxygenation both on skin and tumor surface. Oxyhemoglobin saturation (SO_2) (A), tissue concentration of total hemoglobin (ctTHb) (B), and red blood cell (RBC)

JPET Fast Forward. Published on May 5, 2022 as DOI: 10.1124/jpet.121.001058
This article has not been copyedited and formatted. The final version may differ from this version.

tissue fraction (C) of tumor skin (Sk) and tumor surface (Ts) was monitored by using EPOS system in tumor-bearing mice treated with different doses of sodium pentobarbital and healthy controls. Data are presented as the mean±S.D. ****P ≤0.0001; **P ≤0.01; *P ≤0.05.

A

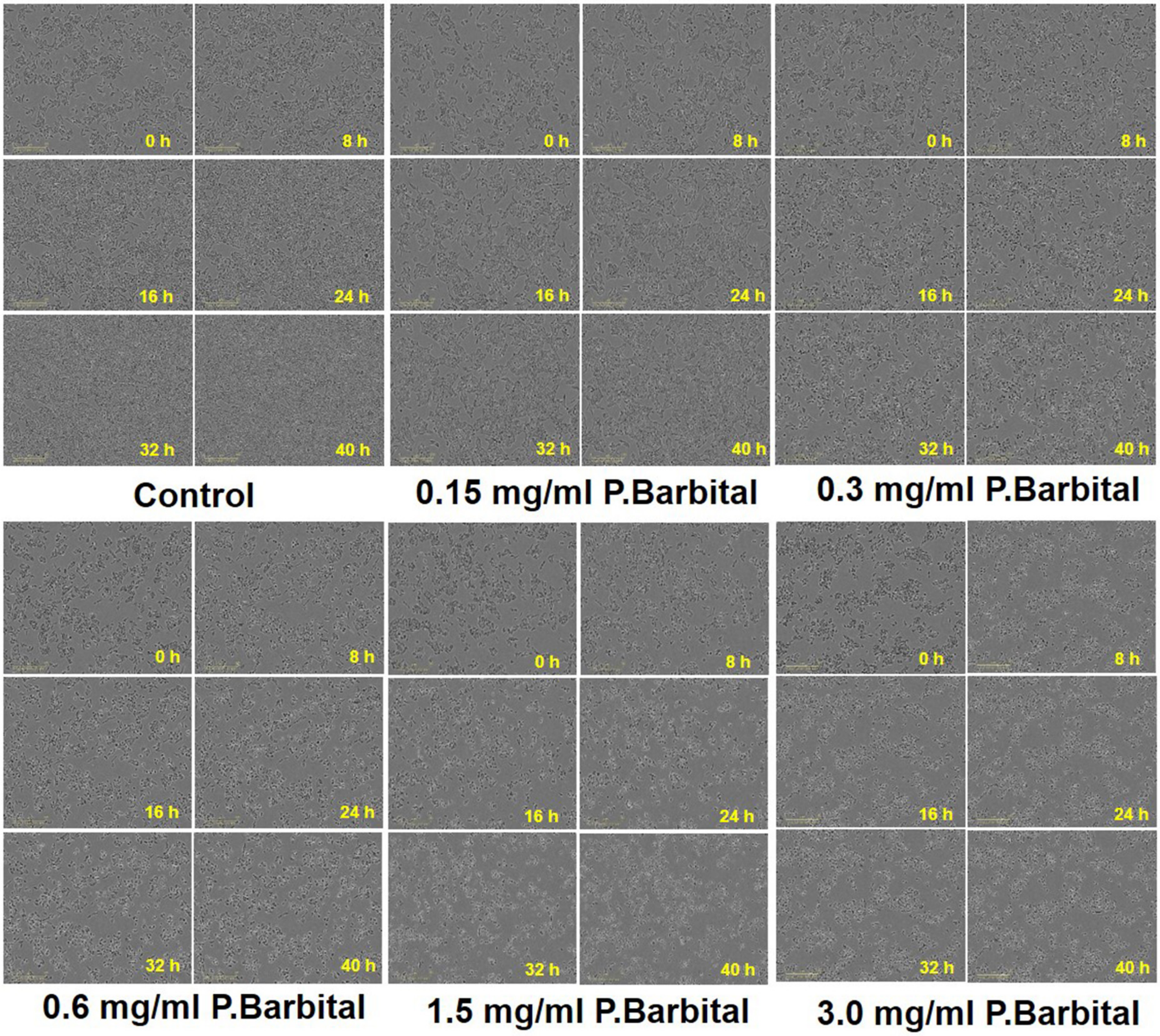

B

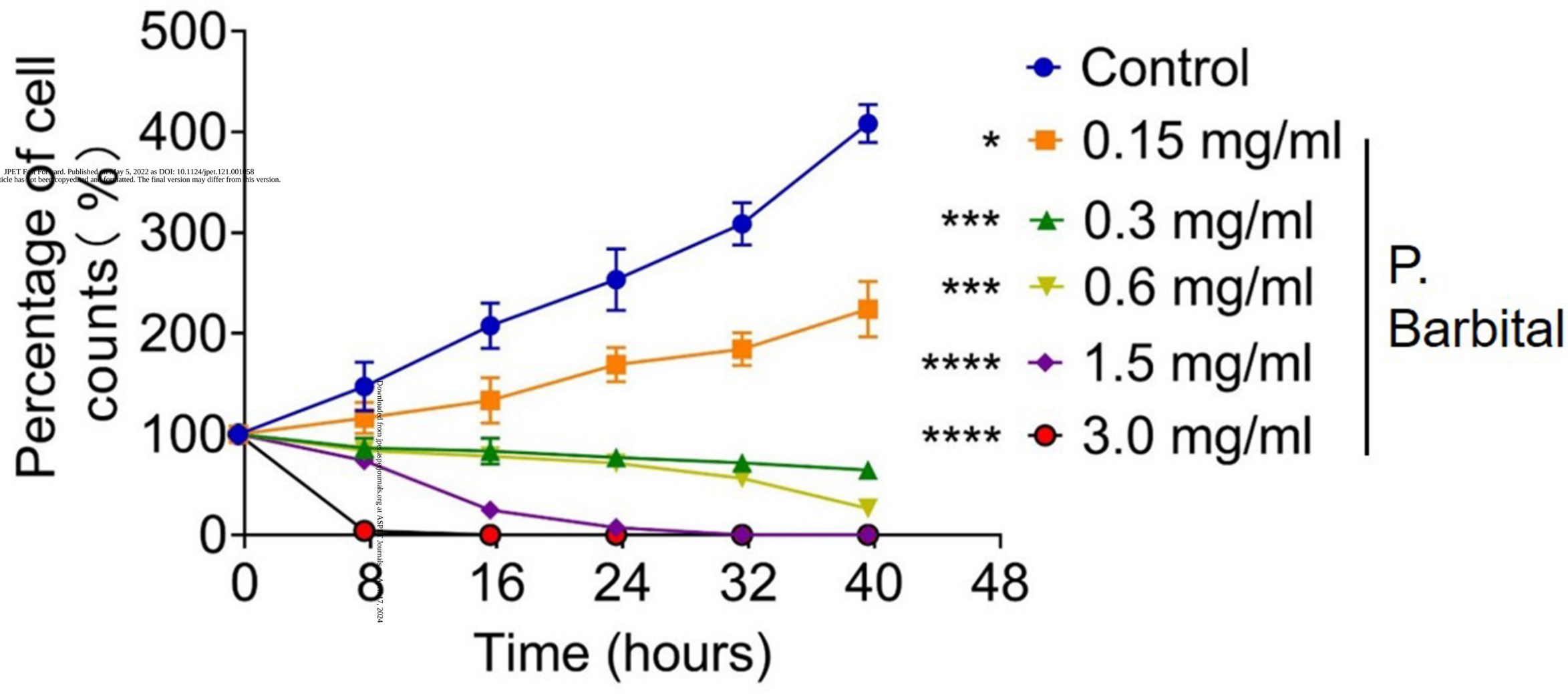

Fig 1

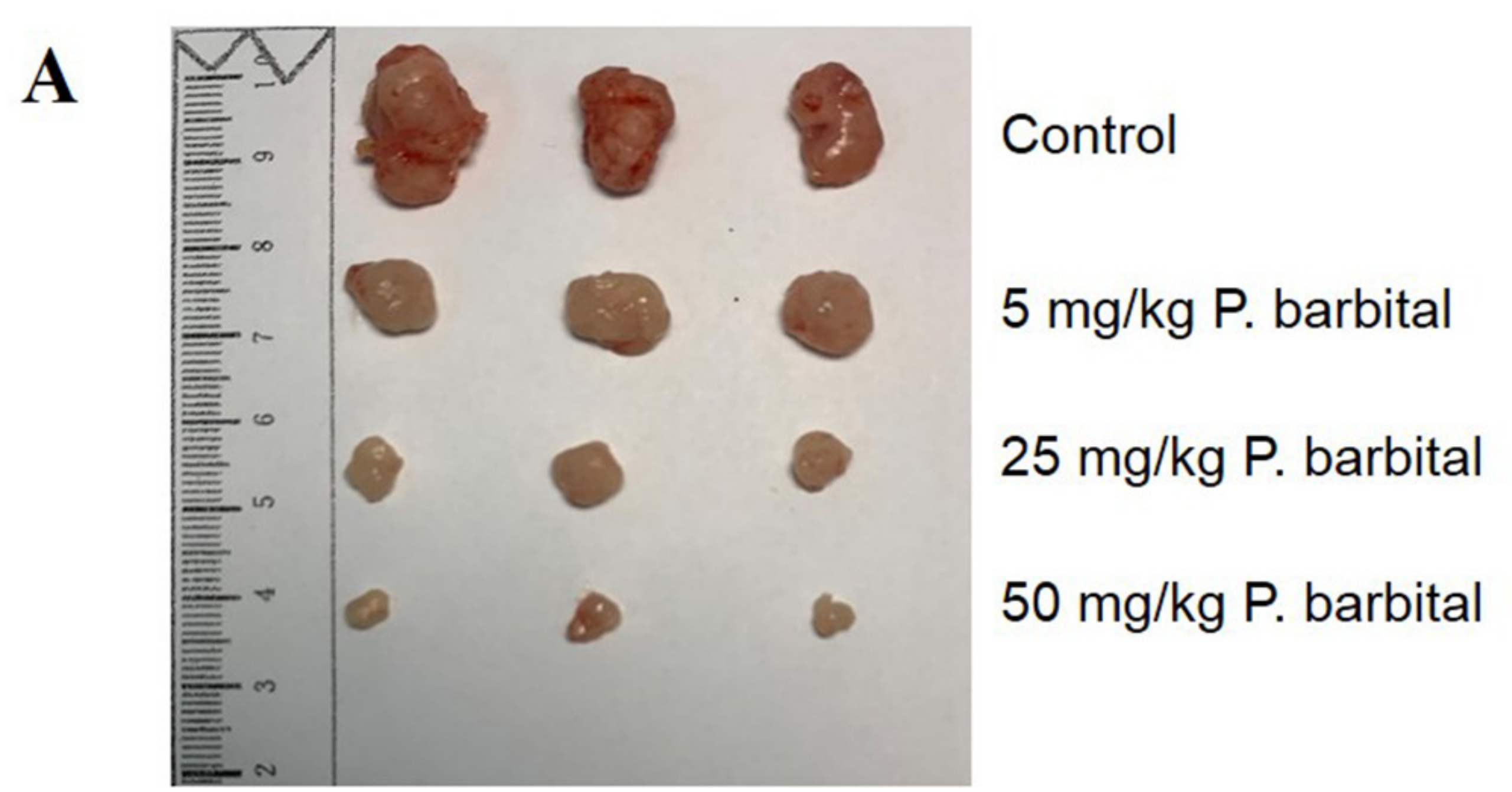

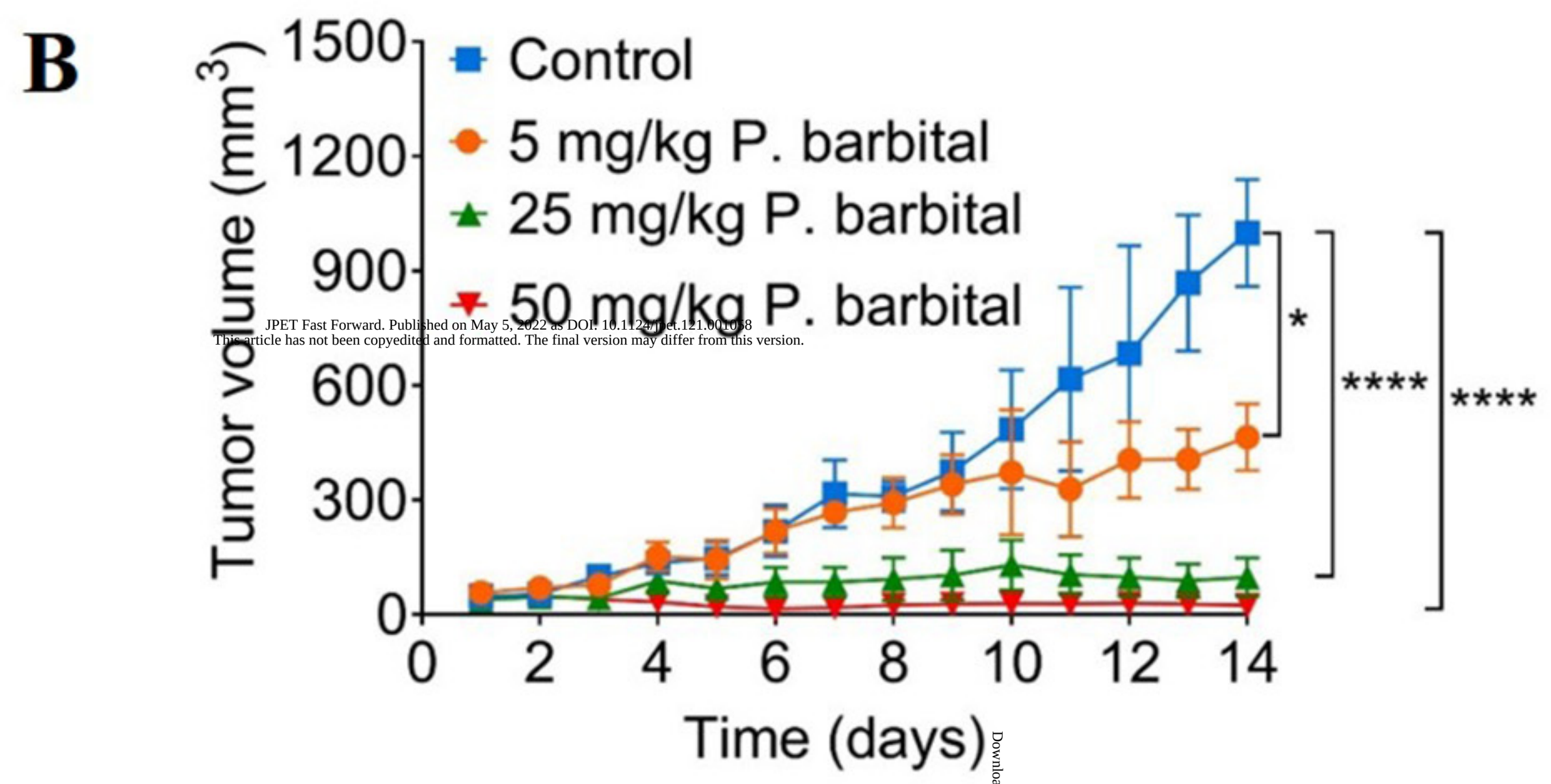

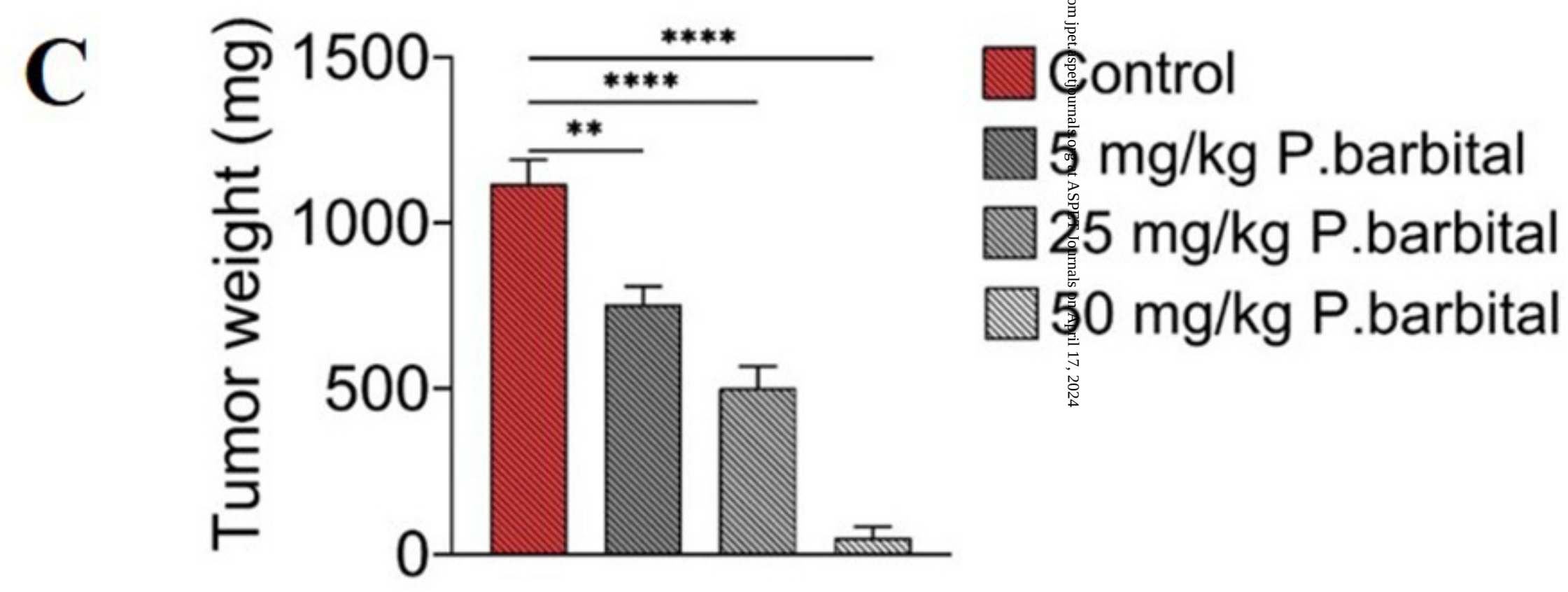

Fig 2

JPET Fast Forward. Published on May 5, 2022 as DOI: 10.1124/jpet.121.001058
This article has not been copyedited and formatted. The final version may differ from this version.

A

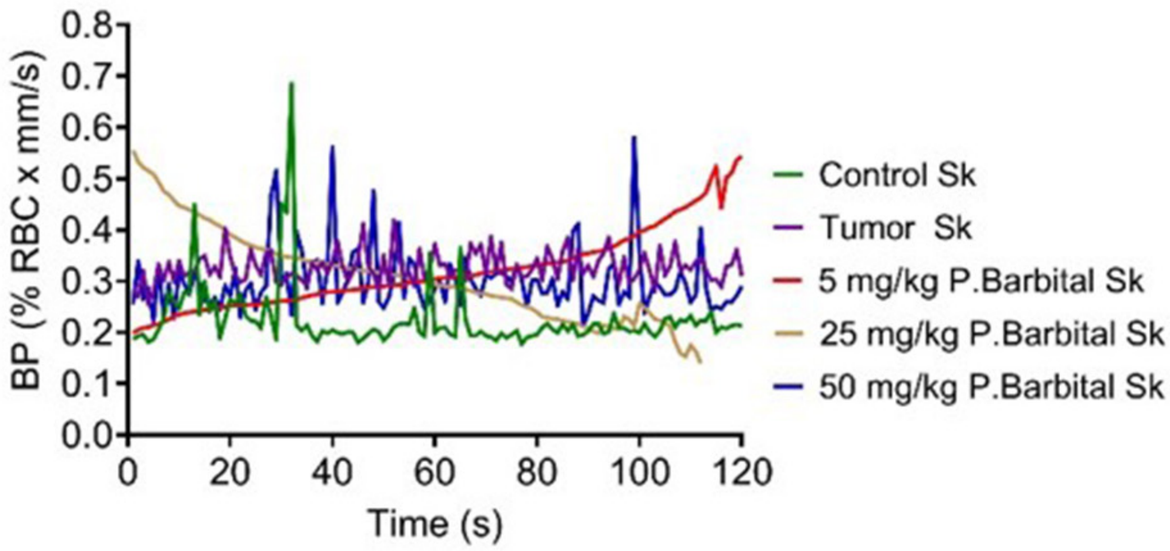

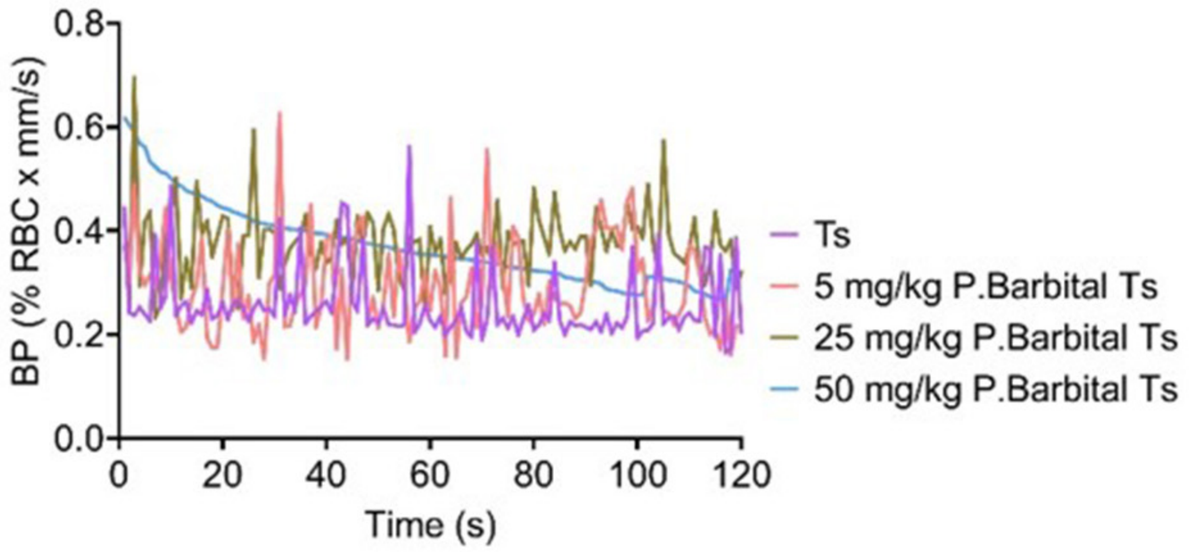

<1 mm/s

B

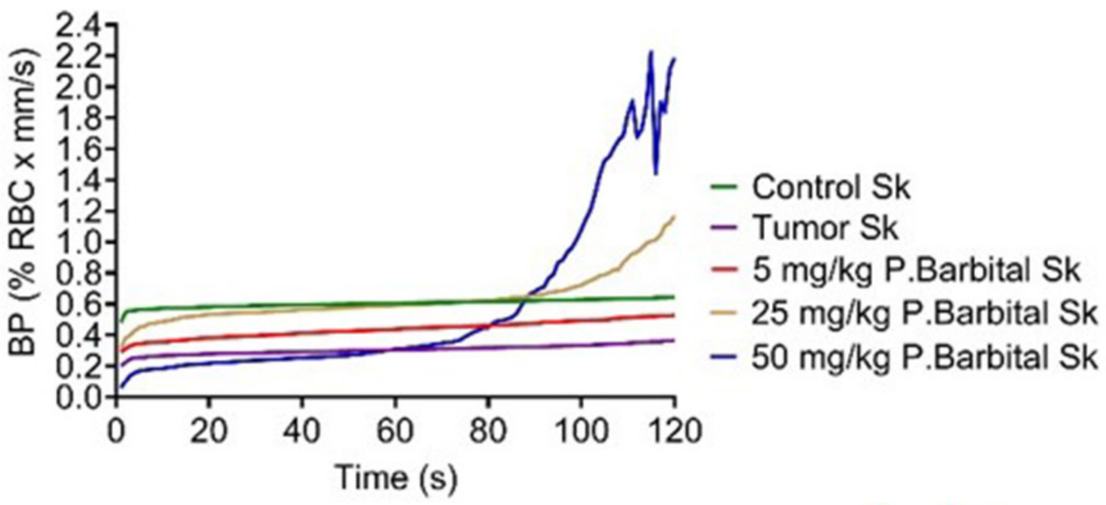

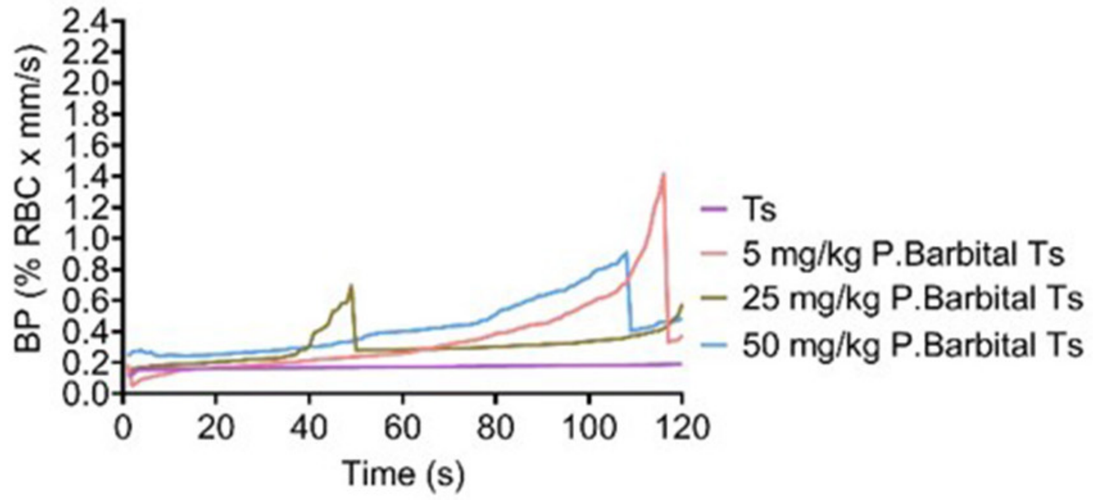

1-10 mm/s

C

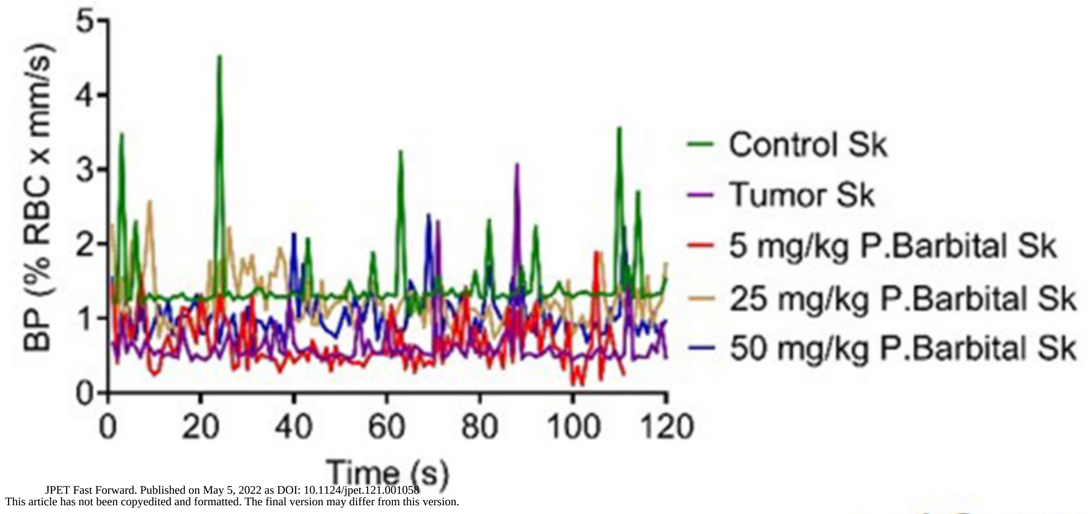

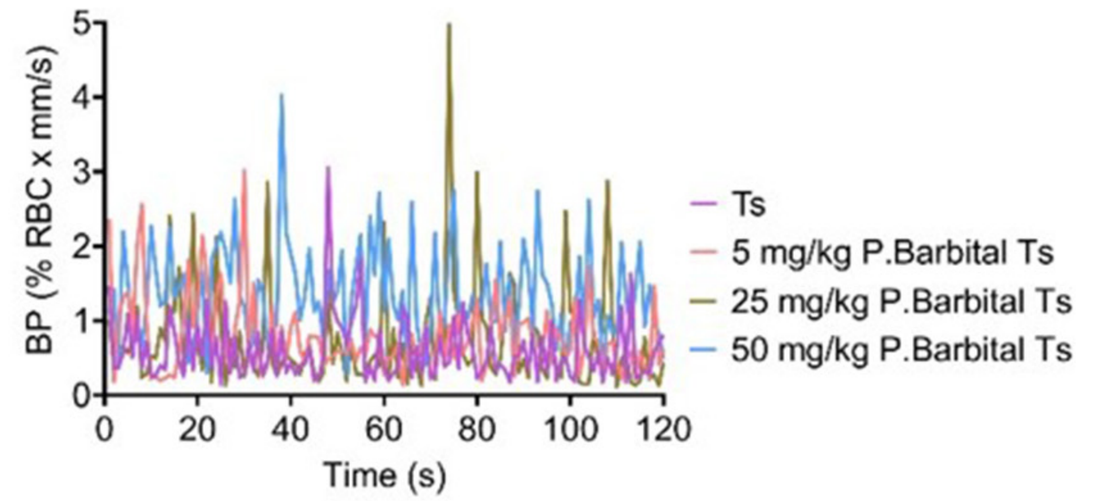

JPET Fast Forward. Published on May 5, 2022 as DOI: 10.1124/jpet.121.001058
This article has not been copyedited and formatted. The final version may differ from this version.

>10 mm/s

D

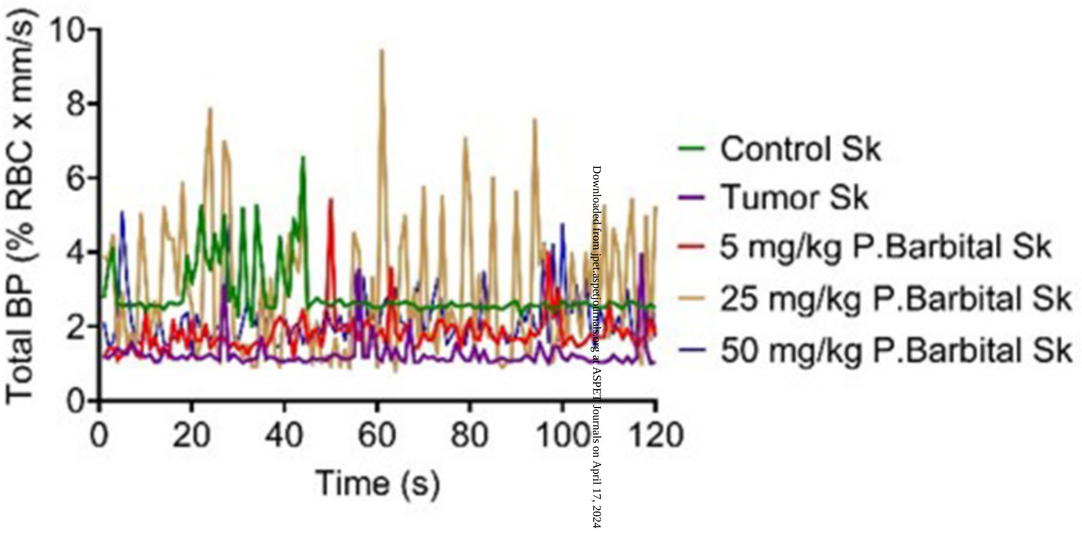

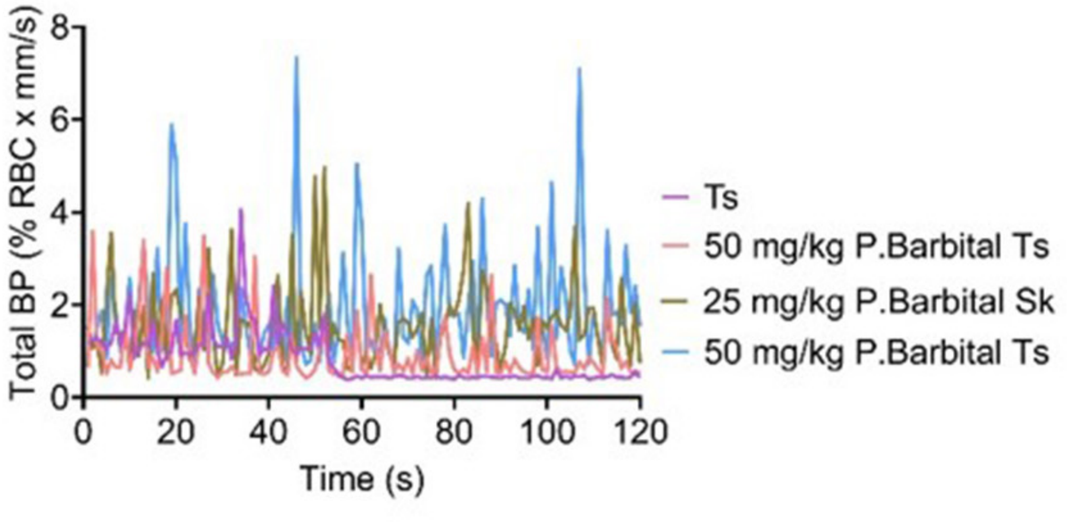

all speed

Fig 3

JPET Fast Forward. Published on May 5, 2022 as DOI: 10.1124/jpet.121.001058
This article has not been copyedited and formatted. The final version may differ from this version.

A

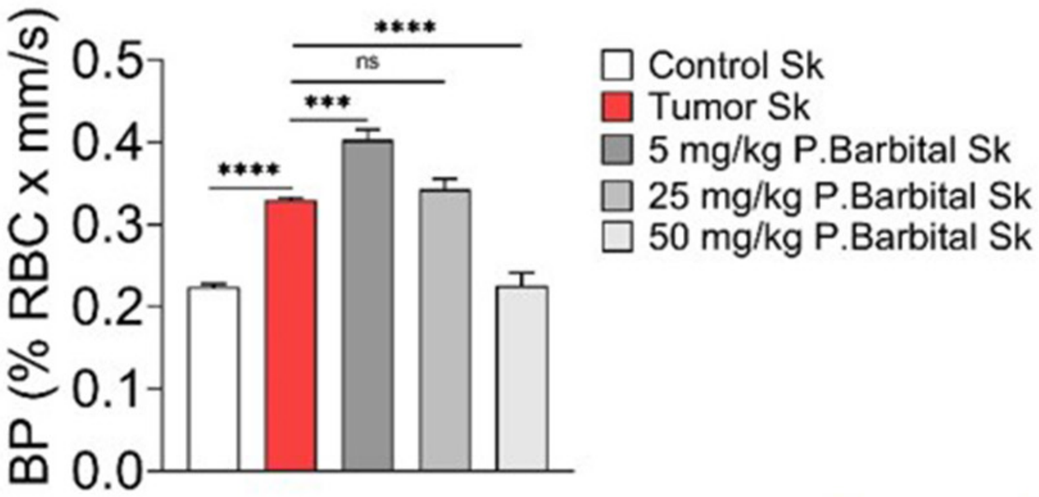

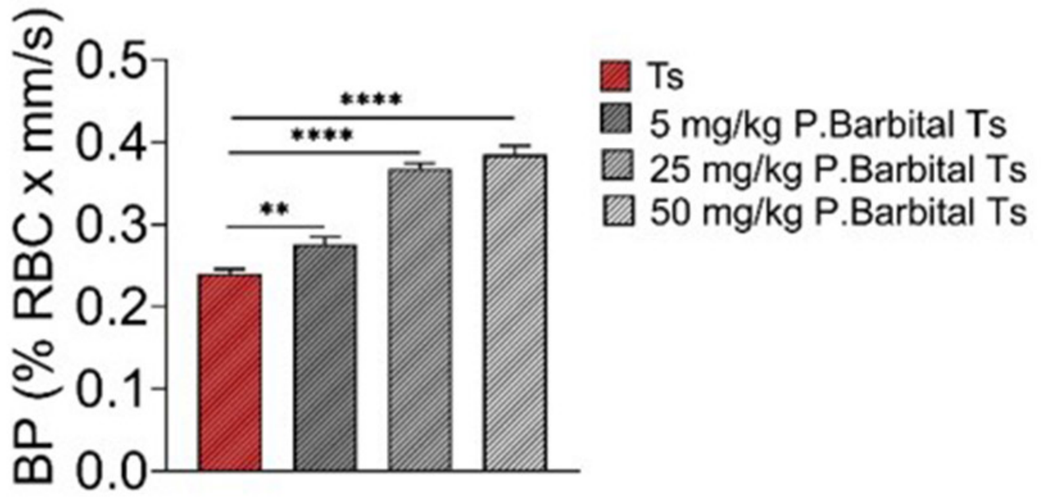

<1 mm/s

B

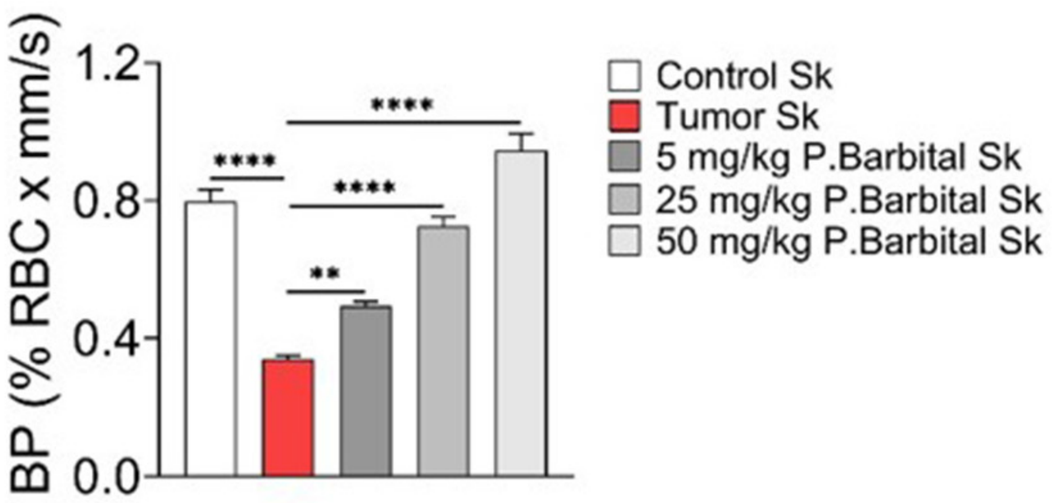

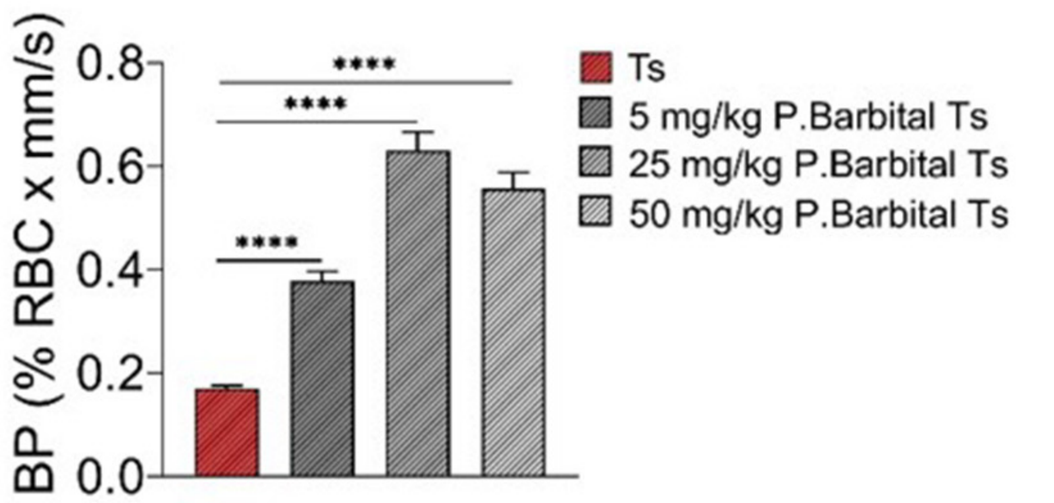

1-10 mm/s

C

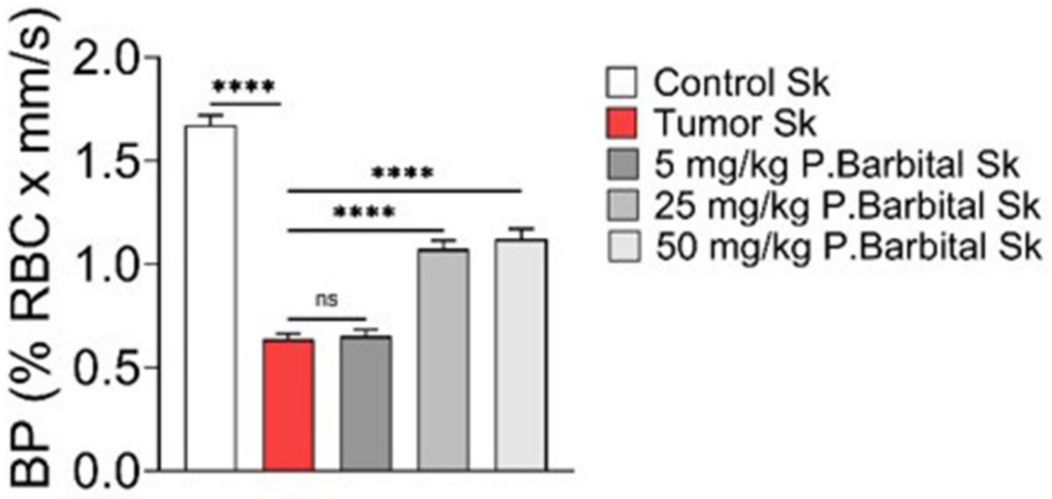

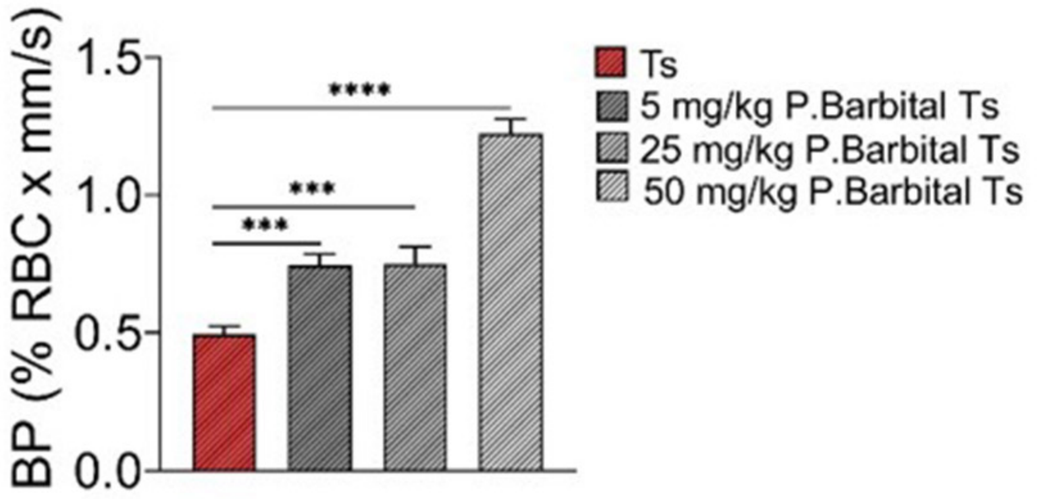

>10 mm/s

D

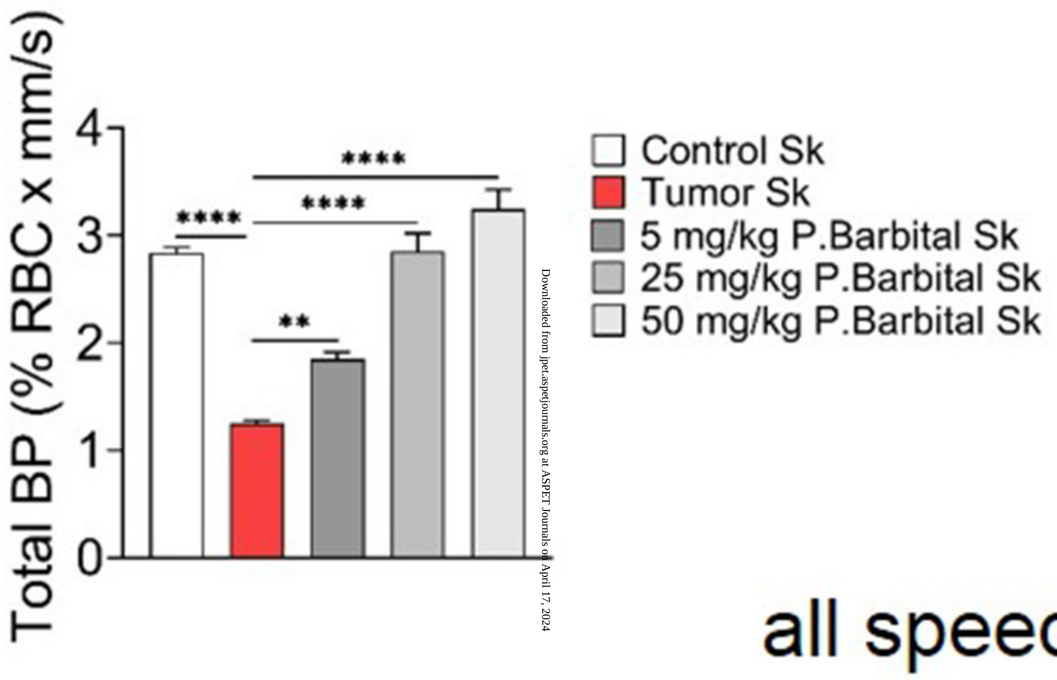

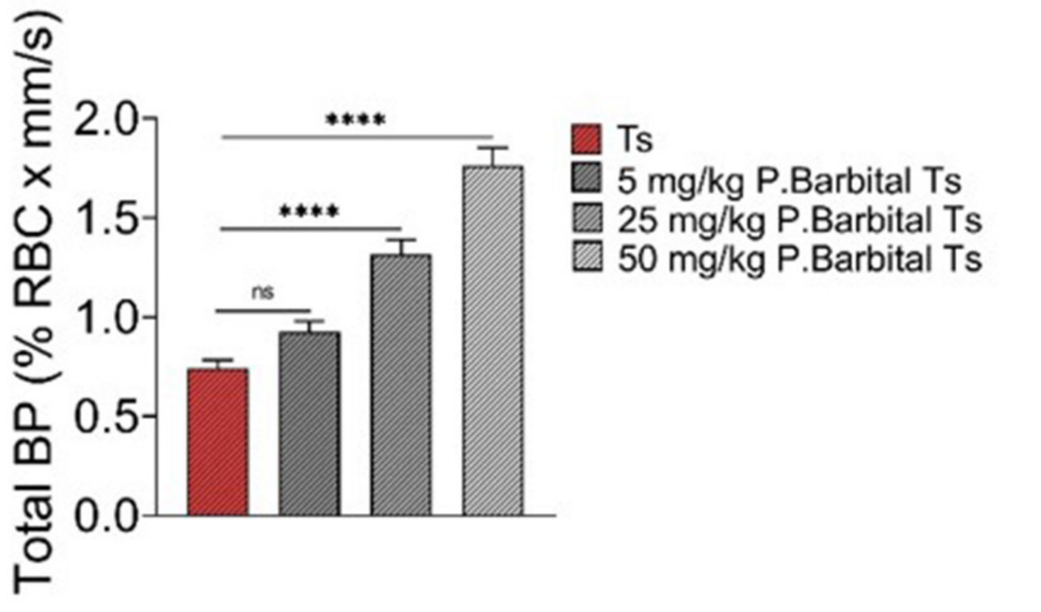

all speed

Fig 4

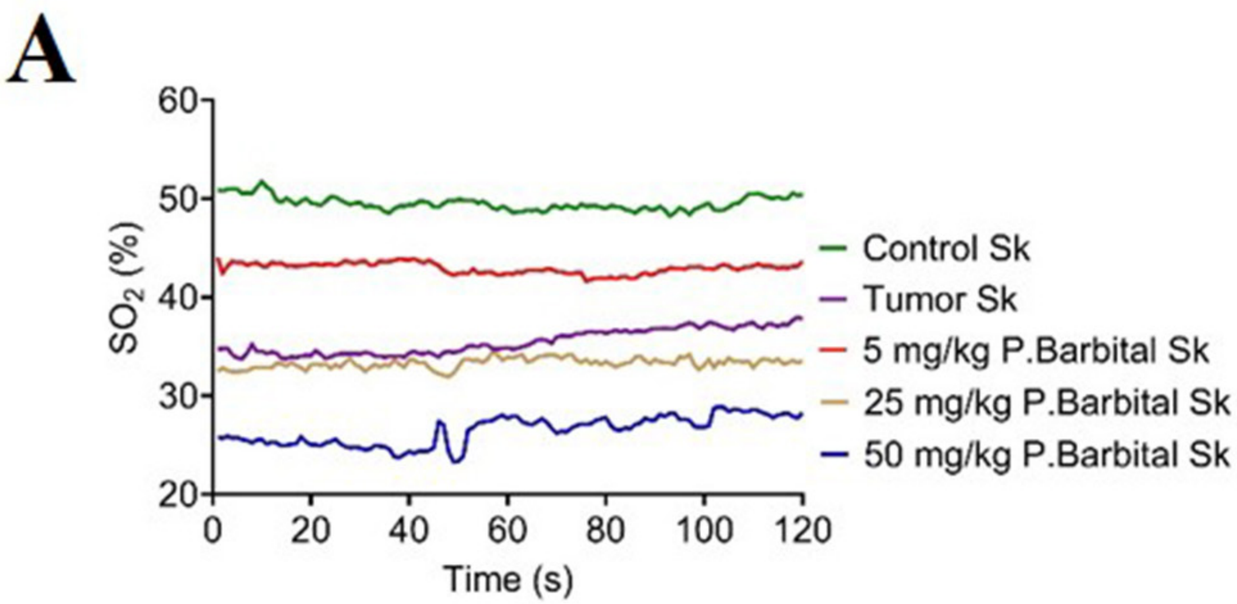

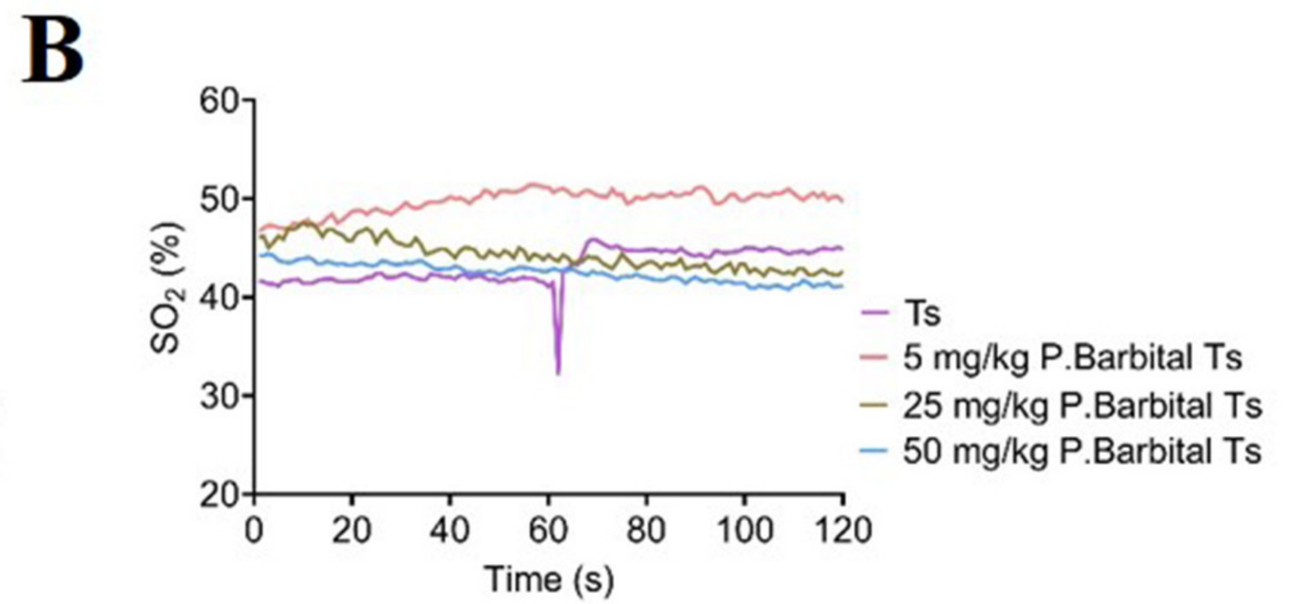

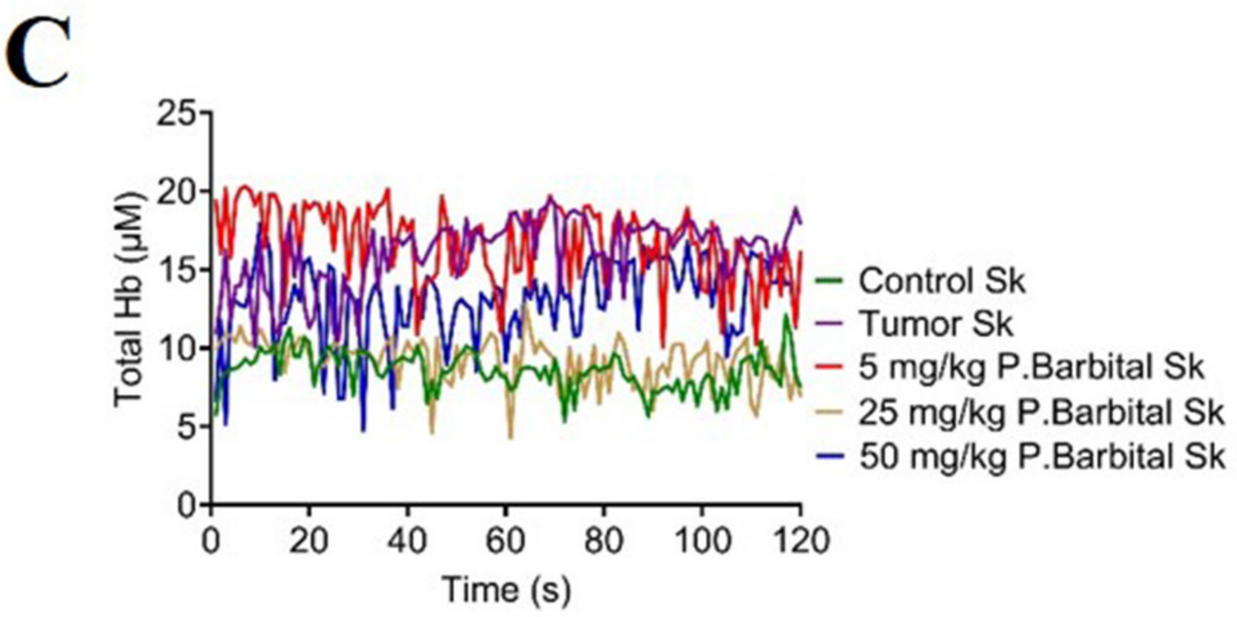

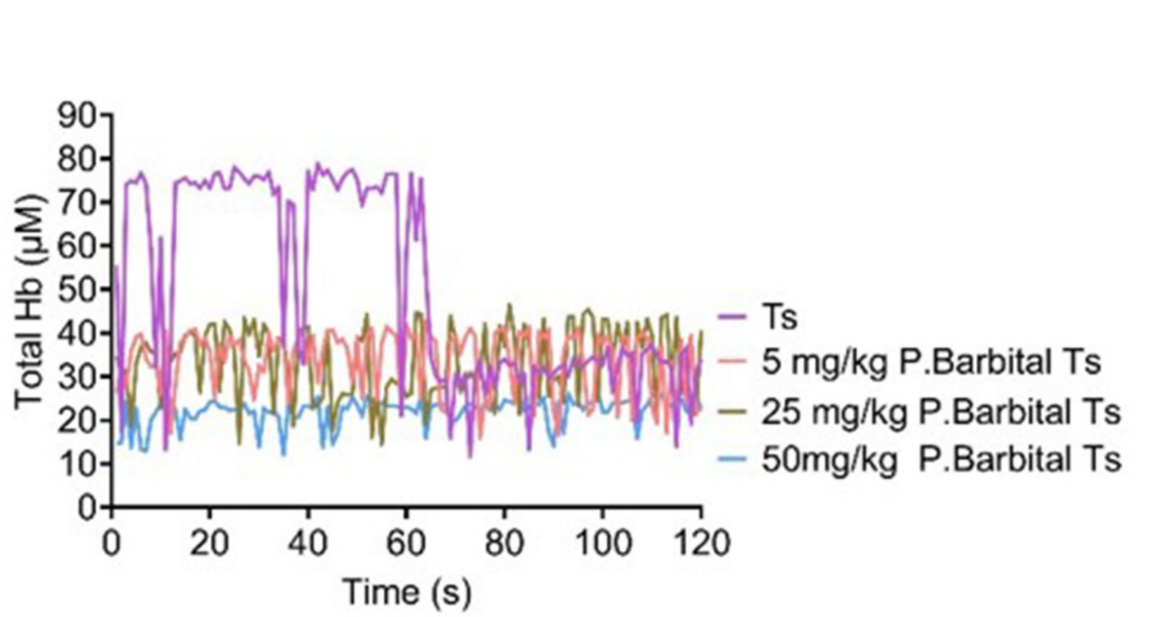

JPET Fast Forward. Published on May 5, 2022 as DOI: 10.1124/jpet.121.001058
This article has not been copyedited and formatted. The final version may differ from this version.

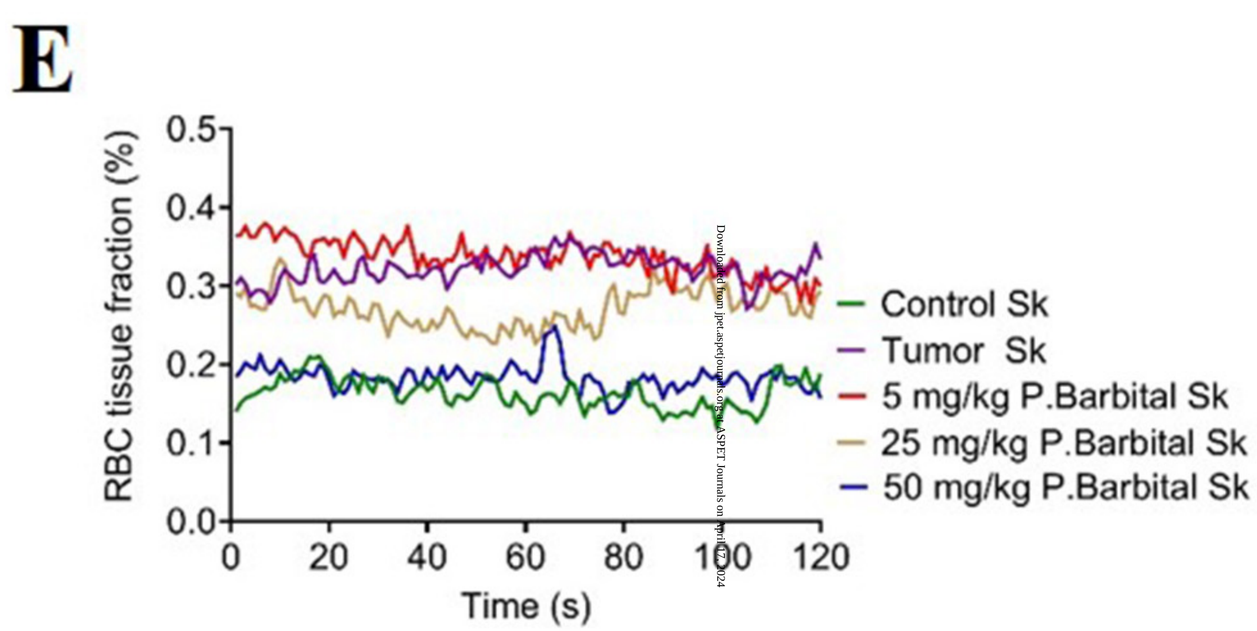

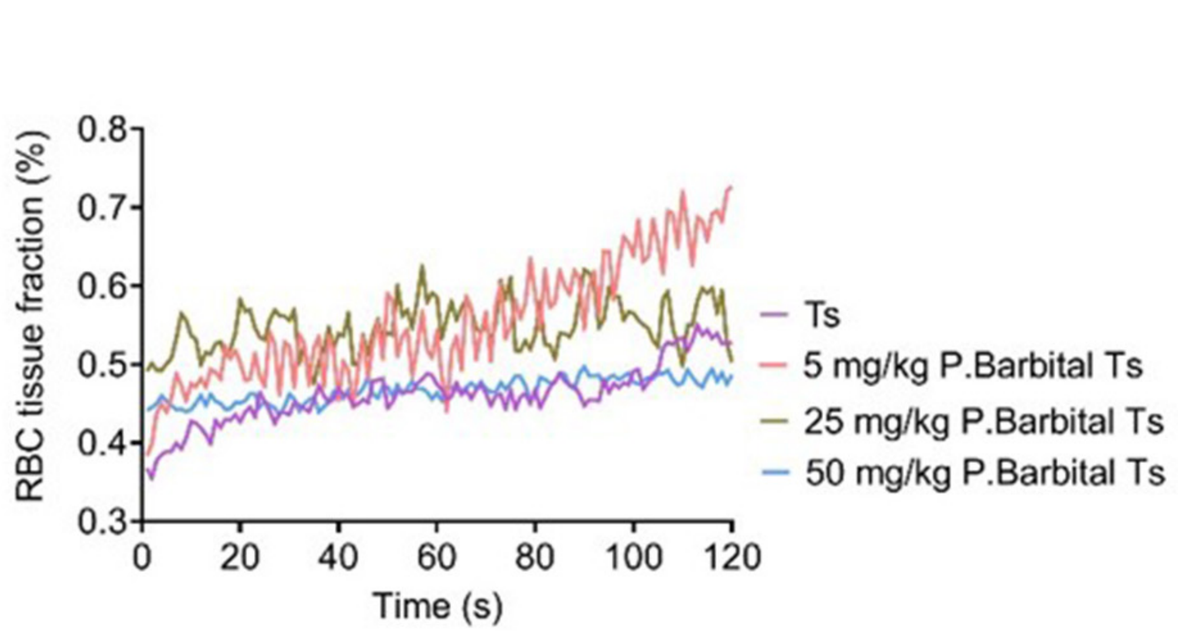

Fig 5

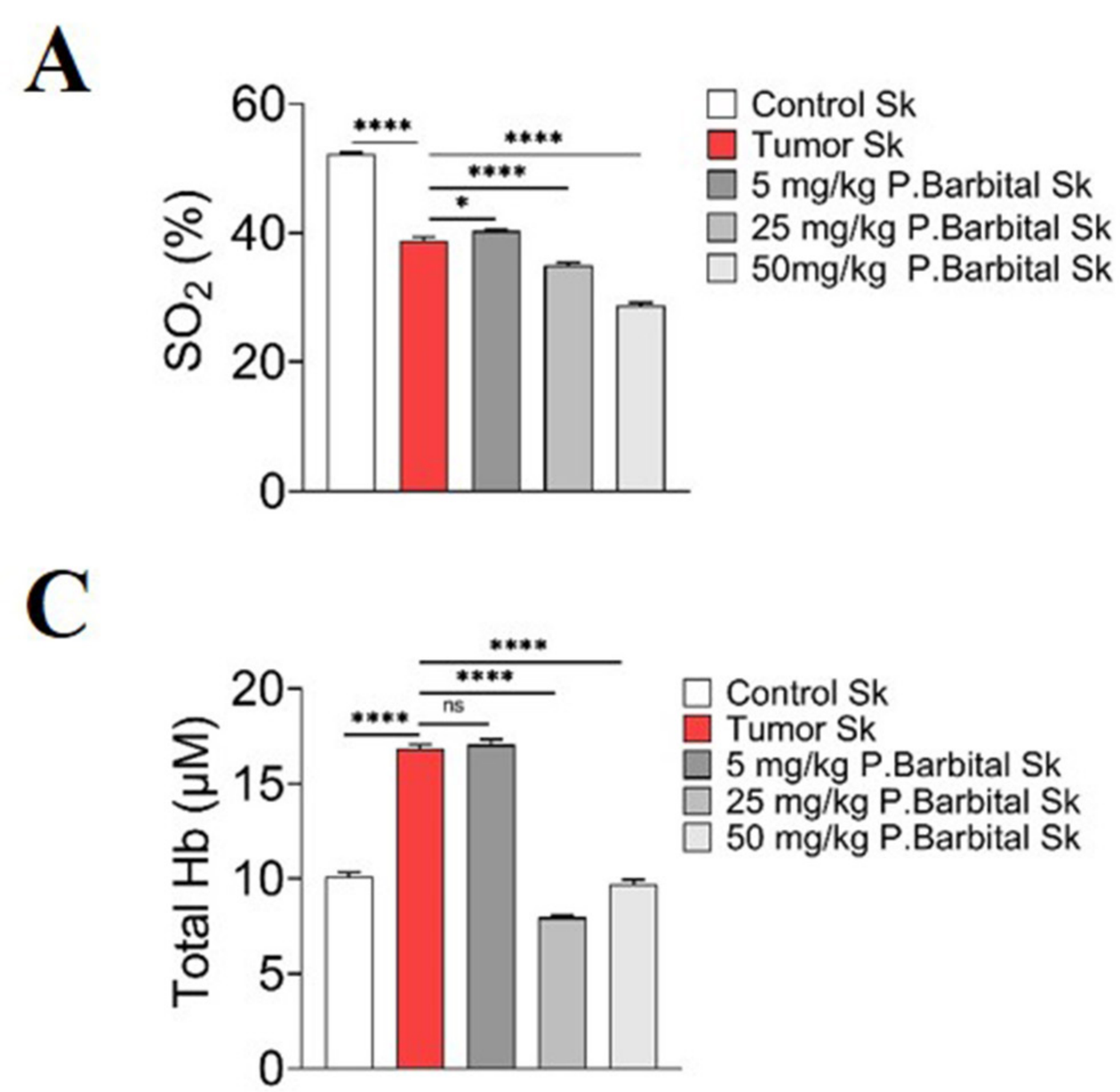

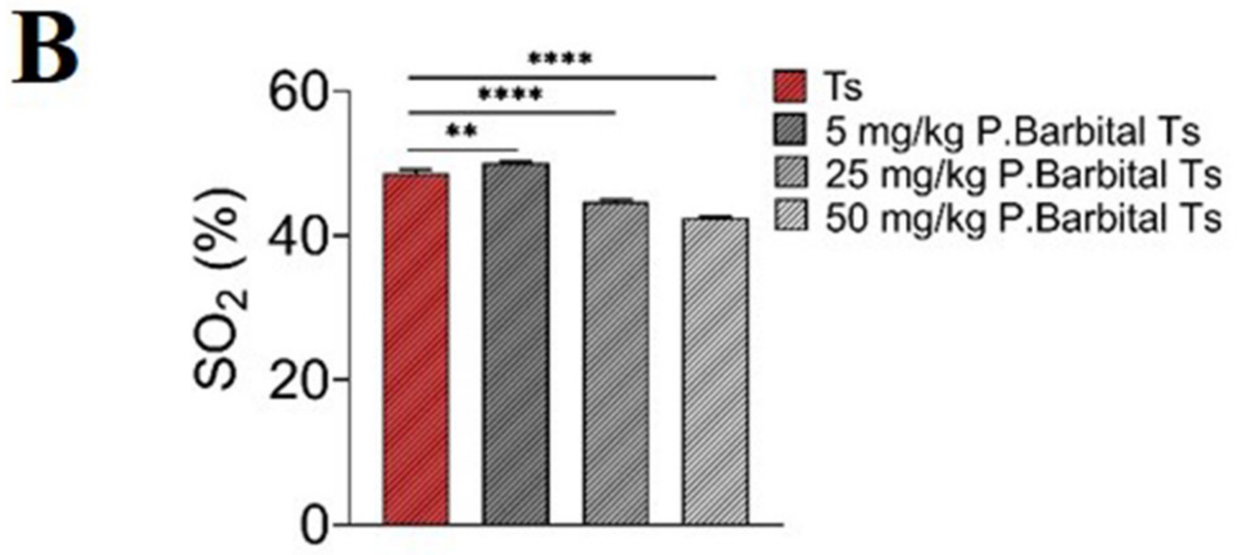

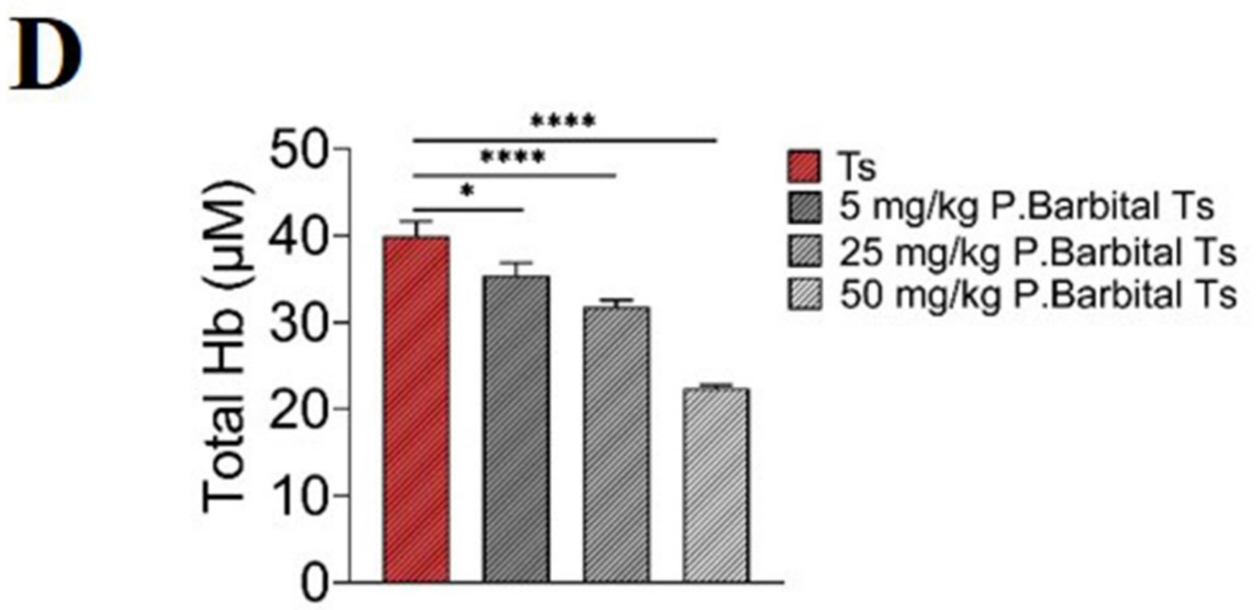

JPET Fast Forward. Published on May 5, 2022 as DOI: 10.1124/jpet.121.001058
This article has not been copyedited and formatted. The final version may differ from this version.

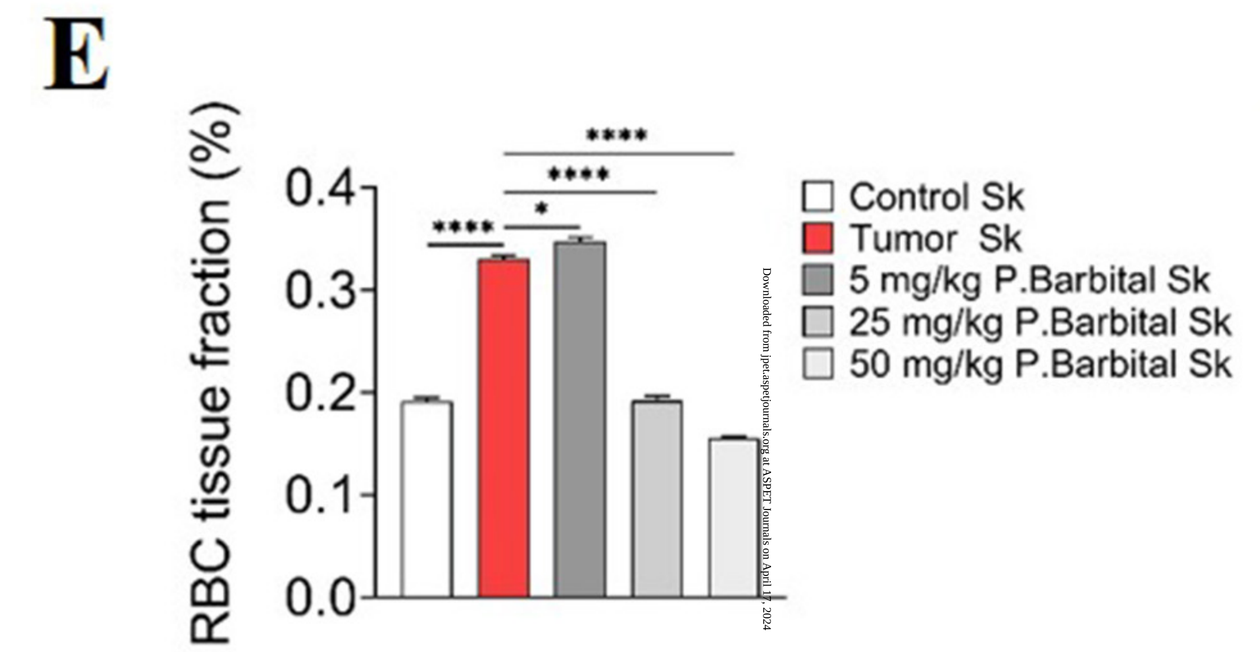

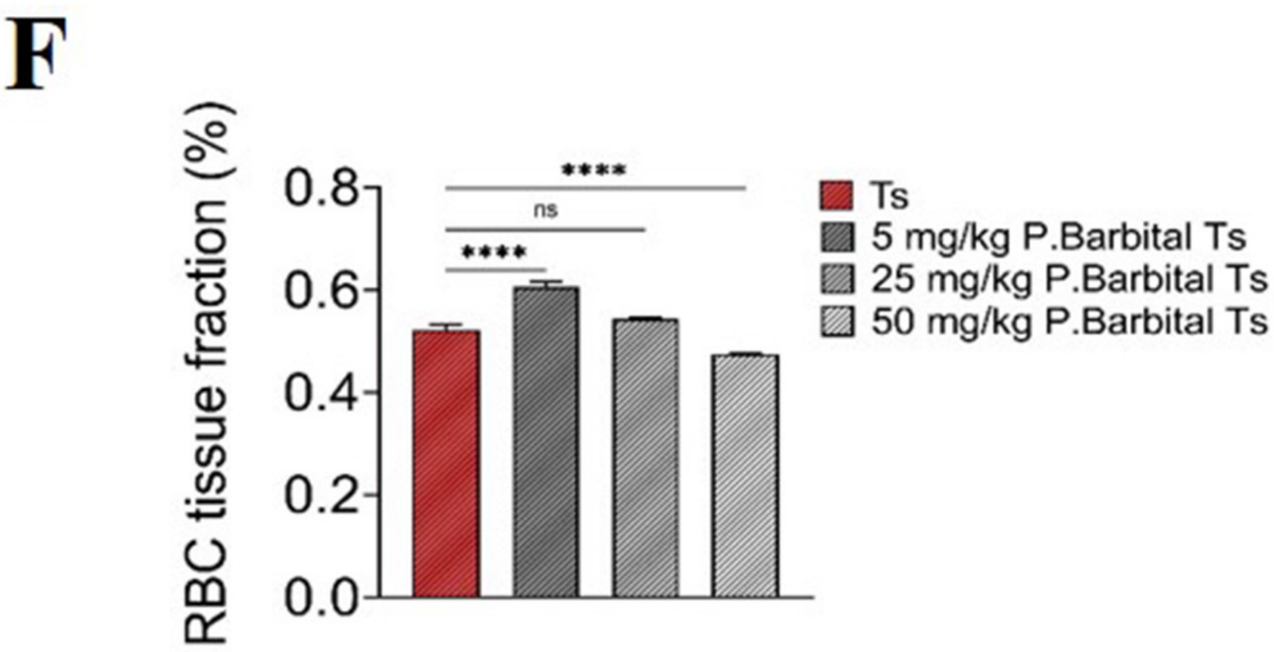

Fig 6